Research Square

Preprints are preliminary reports that have not undergone peer review.
They should not be considered conclusive, used to inform clinical practice,
or referenced by the media as validated information.

Community structure and hidden phylogenetic diversity of marine fungi in the tropical Indian and western Pacific Oceans

Leilei Huang
Guangxi University
Lijia Xu
South China Institute Of Environmental Sciences
Honglei Jiang
Guangxi University
Guangjun Chai
First Affiliated Hospital Zhejiang University
Yuxiao Li
Guangxi University
Sanqiang Gong
gongsanqiang@gxu.edu.cn
Guangxi University
Kefu Yu
Guangxi University

Research Article

Keywords: Marine fungi, hidden diversity, long-read metabarcoding, tropical Indian Ocean, western Pacific Ocean, vertical stratification, environmental drivers, fungal guilds

Posted Date: October 29th, 2026

DOI: https://doi.org/10.21203/rs.3.rs-11293285/v1

License: This work is licensed under a Creative Commons Attribution 4.0 International License.
Read Full License

Additional Declarations: No competing interests reported.

Community structure and hidden phylogenetic diversity of marine fungi in the tropical Indian and western Pacific Oceans

Leilei Huang[a#], Lijia Xu[b#], Honglei Jiang[a], Guangjun Chai[d], Yuxiao Li[a], Sanqiang Gong[a*], Kefu Yu[a,c*]

[a]Guangxi Laboratory on the Study of Coral Reefs in the South China Sea, Coral Reef Research Center of China, School of Marine Sciences, Guangxi University, Nanning, China

[b]South China Institute of Environmental Sciences, The Ministry of Ecology and Environment of PRC, Guangzhou, China

[c]Southern Marine Science and Engineering Guangdong Laboratory (Guangzhou), Guangzhou, China

[d]Department of Laboratory Medicine of the First Affiliated Hospital, Liangzhu Laboratory, Zhejiang University School of Medicine, Hangzhou, China

[#]These authors contributed equally to this work and should be considered co-first authors.

e-mail: gongsanqiang@gxu.edu.cn; kefuyu@scsio.ac.cn

Abstract

Background: Marine fungi remain a poorly understood component of ocean ecosystems despite their potential roles in marine biogeochemical cycling. Here, we investigated fungal diversity, community structure, vertical stratification, and environmental drivers across the tropical Indian and western Pacific Oceans using long-read 28S rRNA gene amplicon sequencing of 113 samples from surface waters, mesopelagic and bathypelagic zones, and sediments.

Results: A total of 46,938 fungal OTUs were clustered, representing 35 phyla, 164 classes, 254 orders, 509 families, 940 genera, and 1,055 species. Ascomycota dominated fungal communities, followed by Basidiomycota, Chytridiomycota, Rozellomycota. Phylogenetic analyses revealed three deeply divergent fungal lineages distinct from currently recognized phyla. Pending further molecular and morphological validation, these lineages were provisionally designated as Candidate.Taichumycota, Candidate.Shizhenmycota, and Candidate.Xihemycota. Their distinct vertical stratification suggested potential ecological differentiation: Candidate.Taichumycota was restricted to surface waters, Candidate.Shizhenmycota was broadly distributed but enriched in surface communities, whereas Candidate.Xihemycota occurred across habitats and was particularly enriched in sediments. Both fungal taxonomic and functional compositions exhibited significant vertical differentiation across habitats ($p < 0.05$), with undefined saprotrophic guilds enriched in sediments and pelagic communities displaying diverse trophic strategies. Surface fungal community composition was jointly shaped by geographic and environmental gradients, with longitude, phosphate, and salinity identified as major predictors. Together, these variables explained 18.6% of the variation in surface fungal community composition.

Conclusions: This study reveals extensive hidden diversity and complex ecological

structuring of marine fungi in the tropical Indian and western Pacific Oceans. The discovery of deeply divergent fungal lineages and habitat-associated shifts in taxonomic and predicted functional composition highlights the underestimated evolutionary diversity and ecological differentiation of marine fungal communities.

Keywords: Marine fungi; hidden diversity; long-read metabarcoding; tropical Indian Ocean; western Pacific Ocean; vertical stratification; environmental drivers; fungal guilds

Background

The ocean represents the largest continuous habitat on Earth and harbors microbial communities that drive global biogeochemical cycles [1–3]. However, most marine microbial research has historically focused on bacteria and archaea, whereas marine fungi have received comparatively less attention [4]. Despite their recognized ecological roles as saprotrophs, parasites, and pathogens, marine fungi were long considered primarily associated with benthic substrates, such as driftwood and seafloor sediments [5, 6]. Recent studies have demonstrated that pelagic fungi are widely distributed throughout the water column across major ocean basins and actively participate in organic matter degradation and nutrient cycling [7, 8]. Functionally, planktonic fungi can degrade complex organic compounds through extracellular enzymatic activities, contributing to carbon, nitrogen, and phosphorus cycling [9–11]. In addition, parasitic chytrids regulate phytoplankton populations and facilitate energy transfer through the "mycoloop", linking primary producers with higher trophic levels [12, 13]. In benthic environments, saprotrophic fungi accelerate organic matter decomposition, while associations with corals, sponges, and algae suggest potential roles in host health and environmental adaptation [14, 15].

Quantitative approaches based on ergosterol extraction and CARD-FISH techniques have further highlighted the ecological importance of oceanic fungi, suggesting that fungal biomass represents a substantial component of marine microbial biomass [4, 16]. High-throughput sequencing targeting fungal marker genes has revealed that Ascomycota and Basidiomycota dominate many marine habitats, while

Chytridiomycota and Rozellomycota are also frequently detected [17, 18]. However, a considerable proportion of environmental fungal sequences cannot be confidently assigned to known taxa and are often difficult to incorporate into diversity assessments, potentially resulting in an incomplete understanding of marine fungal diversity [19, 20]. Although marine fungi are increasingly recognized as important components of ocean ecosystems, their large-scale biogeographic patterns and the environmental drivers shaping their distribution remain incompletely understood [4]. Previous studies have shown that marine fungal communities respond to various environmental gradients, including temperature, salinity, nutrient availability, and productivity-related variables [21, 22]. However, most existing studies have been conducted at regional scales or within specific habitats, such as polar waters, coastal environments, sediments, and hydrothermal systems [17, 18, 21, 23]. These studies have provided valuable insights into habitat-specific patterns of marine fungal communities. For example, benthic fungal communities in the Baltic Sea have been associated with variations in depth, salinity, and resource availability [24], while coastal studies have suggested that geographic gradients may contribute to differences in fungal community composition [25]. Nevertheless, whether geographic and environmental factors consistently shape marine fungal communities across broad oceanic regions and complex vertical habitats remains largely unresolved.

The tropical Indian and western Pacific Oceans represent one of the most environmentally heterogeneous marine regions, characterized by pronounced gradients in temperature, salinity, nutrient availability, productivity, and water-column structure [23, 26]. The Indian Ocean is influenced by large-scale monsoon-driven circulation patterns, while the western Pacific Ocean is shaped by complex boundary currents and strong land–sea–air interactions, generating substantial spatial and environmental

variability [27, 28]. These characteristics provide an ideal natural setting for investigating how marine fungal communities respond to broad-scale geographic gradients and vertical habitat differentiation. In this study, we conducted a large-scale survey of fungal communities across 113 samples collected from stations in the tropical Indian Ocean and western Pacific Ocean, covering multiple multiple oceanic habitats, including surface, mesopelagic, bathypelagic, and sediment environments. Using long-read 28S rRNA gene amplicon sequencing combined with a curated multi-source reference database, we aimed to: (1) characterize the taxonomic diversity and phylogenetic breadth of marine fungi across this comparatively underexplored biogeographic region; (2) identify key geographic and environmental drivers shaping fungal community structure; and (3) infer potential ecological functions through predicted functional guilds, thereby improving our understanding of marine fungal diversity, distribution patterns, and ecological roles.

Methods

Sampling regions and sample collection

Sampling was conducted during two oceanographic cruises in the tropical Indian Ocean and the western Pacific Ocean between September 11 and November 30, 2023. A total of 113 samples were collected, spanning latitudes from 12.01°S to 21.78°N and longitudes from 82.68°E to 150.00°E, thereby covering typical tropical and subtropical marine environmental gradients (Figure 1). A conductivity–temperature–depth (CTD) rosette system was deployed at each station to characterize water-column structure and determine sampling depths. Based on vertical distribution, samples were categorized into four habitat types: surface waters (0–200 m, n = 90), mesopelagic waters (200–1000 m, n = 11), bathypelagic waters (1000–4000 m, n = 8), and sediments (n = 4). Seawater samples were collected using Niskin bottles (12 L) mounted on a CTD-rosette

system. Approximately 50 L of seawater was collected per sample, and microbial biomass was concentrated by sequential filtration. Water samples were filtered through a 0.22 μm pore-size filter (PES membrane, PALL Laboratory) to retain microbial communities. Filtration was performed using a Masterflex peristaltic pump, with a filtration volume of approximately 2–5 L per filter depending on clogging conditions. The filters were then placed in sterile 15 mL Falcon tubes and immediately stored at −80°C until DNA extraction. To avoid cross-contamination between samples, the filtration system was thoroughly cleaned with 10% bleach and filtered seawater between samples. Sediment samples were collected using a box corer. Surface sediments (0–10 cm) were subsampled from the center of each core under sterile conditions to minimize edge contamination. All sediment samples were preserved at low temperature immediately after collection and transported to the laboratory for further analysis.

Environmental data collection

During sampling, in situ environmental measurements were conducted at all stations to characterize local oceanographic conditions. Tmperature, salinity, and depth were recorded using a CTD profiler (Idronaut, Italy). Dissolved oxygen (DO) was measured using a YSI 6600V2-02 multiparameter instrument (Xylem-YSI, Yellow Springs, OH, USA). Prior to deployment, the YSI instrument was calibrated following the manufacturer's recommended two-point procedure using sodium sulfite solution for zero-oxygen calibration and water-saturated air for full-scale calibration [29, 30]. Inorganic nutrients, including nitrite (NO_2^-), nitrate (NO_3^-), ammonium (NH_4^+), and phosphate (PO_4^{3-}), were analyzed using a Lachat QC8500 flow injection autoanalyzer (Lachat Instruments, Loveland, CO, USA) according to standard oceanographic protocols (GB/T 12763.6-2007) (Additional file 1).

To investigate large-scale environmental drivers of marine fungal diversity and community composition, five oceanographic variables were further compiled from publicly available global environmental raster datasets (Additional file 2): sea surface temperature (SST, °C), sea surface salinity (PSU), chlorophyll *a* concentration (Chl *a*, mg m^{-3}), nitrate concentration (μmol L^{-1}), and phosphate concentration (μmol L^{-1}). SST data were downloaded from MODIS Aqua and Terra satellite products provided by the NASA Ocean Color database (https://oceancolor.gsfc.nasa.gov/) at a spatial resolution of approximately 4 km, whereas salinity, Chl a, nitrate and phosphate data were obtained from Bio-ORACLE v2.1 (version 2.1) [31] at a spatial resolution of 0.083° (approximately 9–10 km). Environmental raster datasets were downloaded as quality-controlled NetCDF files and processed using the xarray package in Python. Environmental values for each sampling station were extracted using bilinear interpolation based on geographic coordinates. When multiple temporal layers were available, temporal averages were calculated to generate climatological environmental estimates before spatial extraction. These long-term environmental averages were used to minimize the influence of short-term fluctuations and facilitate comparisons among sampling locations. However, they may not fully represent instantaneous environmental conditions during sampling cruises.

DNA extraction and amplicon sequencing

Total genomic DNA was extracted from sediment samples using the PowerSoil DNA Isolation Kit (MoBio Laboratories, Carlsbad, CA, USA) following the manufacturer's protocol. For seawater samples, microbial biomass retained on 0.22 μm polyethersulfone (PES) membrane filters (PALL Laboratory) was used for DNA extraction. DNA quality was assessed by 1% (w/v) agarose gel electrophoresis. DNA concentration was quantified using a Qubit® 3.0 Fluorometer (Life Technologies,

United States), and DNA purity was evaluated using a NanoDrop™ 2000 Spectrophotometer (Thermo Scientific, United States). All DNA samples were stored at −20°C until further use.

PCR amplification of the fungal 28S rRNA gene region was performed using the primers LROR_F (5'-CCGCTGAACTTAAGCATATCAATA-3′) and LR5-F (5′-CGATCGATTTGCACGTCAGA-3′) [32]. Each 20 μL reaction contained 4 μL of 5× FastPfu Buffer, 2 μL of 2.5 mM dNTPs, 0.8 μL of each primer (5 μM), 0.4 μL of TransStart FastPfu DNA Polymerase (TransGen Biotech, Beijing, China), approximately 10 ng of template DNA, and nuclease-free water. PCR cycling conditions were as follows: initial denaturation at 95°C for 5 min; 30 cycles of denaturation at 95°C for 30 s, annealing at 58°C for 30 s, and extension at 72°C for 45 s; followed by a final extension at 72°C for 10 min.

PCR products were verified by 2% agarose gel electrophoresis and quantified using a QuantiFluor™-ST fluorometer (Promega, USA). Equimolar amounts of qualified PCR products were pooled for library construction following the PacBio standard protocol with sample-specific barcodes. Sequencing was performed on the PacBio Sequel II platform using Circular Consensus Sequencing (CCS) technology.

Data Processing and Analysis

Raw CCS sequences for each sample were obtained from the PacBio platform and imported into QIIME 2 (version 2024.10) [33] for downstream analyses. Primer sequences were removed using Cutadapt (version 5.0) [34]. Quality filtering was performed using the filterAndTrim function in the DADA2 R package (version 1.30.0) [35], where reads containing ambiguous bases, expected errors greater than five, low-complexity sequences, or lengths outside the range of 800–1400 bp were discarded, and PhiX sequences were removed. This step was used exclusively for read quality control

and not for amplicon sequence variant inference. Subsequently, high-quality reads were clustered into operational taxonomic units (OTUs) at 97% sequence similarity using the cluster-features-de-novo command in VSEARCH (version 2.22.1) [36] and the most abundant sequence in each OTU was selected as the representative sequence for downstream analyses.

Taxonomic classification was initially conducted using a custom-curated fungal 28S rDNA reference database (Additional file 3) designed for LSU-based fungal taxonomy and containing over 200,000 quality-controlled annotated fungal sequences. Classification was performed with the q2-feature-classifier plugin using a Naïve Bayes approach. OTUs unassigned at the phylum level were further aligned using BLASTn [37] against the custom 28S rDNA database. If necessary, they were also aligned against the NCBI NT_EUK database (https://ftp.ncbi.nlm.nih.gov/blast/db/). For phylum-level unclassified OTUs with an abundance greater than three reads, phylogenetic analyses were performed. Long 28S rDNA reference sequences (>1400 bp) representing major fungal phyla, with Stramenopiles as outgroups, were combined with the OTU sequences and aligned using MAFFT (version 7.525) [38]. Maximum likelihood (ML) phylogenetic trees were constructed in IQ-TREE (version 1.6) [39] under the GTR+F+I+G4 model with 1,000 bootstrap replicates and the Shimodaira–Hasegawa approximate likelihood ratio test (SH-aLRT), while Bayesian inference (BI) analyses were performed in MrBayes (version 3.2) [40] with 2 million MCMC generations using the same model. As ML and BI trees were nearly identical, only the ML tree is presented.

Alpha diversity indices, including Observed OTUs, Shannon index, Simpson index, Inverse Simpson index, and Pielou's evenness, were calculated using the R packages phyloseq, vegan, and ggplot2 [41]. Beta diversity was evaluated with Bray–Curtis dissimilarity and visualized through principal coordinate analysis (PCoA). The

relationships between environmental and geographic variables and fungal diversity were evaluated using regression analyses. Linear regression was used to calculate R^2 values, and generalized additive models (GAMs) were applied to assess potential nonlinear relationships [42, 43]. Redundancy analysis (RDA) was performed using the vegan package in R to evaluate the contributions of environmental and geographic variables to surface fungal community composition [44]. Geographic variables (longitude and latitude) and environmental variables (SST, salinity, chlorophyll *a*, nitrate, and phosphate) were included as explanatory variables. The significance of RDA models and individual predictors was assessed using permutation tests (999 permutations). Partial RDA and variation partitioning were further performed to separate the independent and shared contributions of environmental and geographic variables [44]. Marginal effects of individual predictors were evaluated using separate RDA models [44]. Fungal functional guilds were predicted using FUNGuild [45] in Python (version 3.10.14), which classifies fungi based on ecological traits such as trophic mode, nutritional type, and host association. Analysis code and scripts for data processing are provided in Additional file 4.

Results

Diversity of fungi in the tropical Indian and western Pacific Oceans

Amplicon sequencing of the 28S rRNA gene was performed on 113 samples collected across the tropical Indian and western Pacific Oceans. A total of 2,225,480 high-quality sequences were obtained, which clustered into 46,938 fungal OTUs at a 97% similarity threshold. These fungal OTUs assigned to 35 phyla, 164 classes, 254 orders, 509 families, 940 genera, and 1,055 species (Additional files 5-7). At the phylum level (Figure 2; Additional file 8), fungal communities were dominated by Ascomycota

(52.84% of total OTUs), followed by Basidiomycota (16.67%). Chytridiomycota (7.04%) and Rozellomycota (6.56%) were also abundant, whereas unclassified fungi accounted for 7.44% of all OTUs, suggesting substantial previously uncharacterized fungal diversity in the tropical Indian and western Pacific Oceans.

Phylogenetic analysis of the amplified 28S rRNA region revealed three distinct fungal clades that did not fall within any currently recognized fungal phylum (Figure 3, Table1). Candidate.Taichumycota formed an independent lineage sister to Aphelida, whereas Candidate.Shizhenmycota and Candidate.Xihemycota together formed a monophyletic group that was recovered as sister to Zoopagomycota. These closest known relatives were subsequently used as reference sequences for pairwise comparisons. Within Candidate.Taichumycota, pairwise sequence identities ranged from 84.6% to 92.6% (coverage 97.2–99.6%), whereas comparisons with Aphelida reference sequences showed substantially lower identities (68.4–69.3%) and coverage (95.5–97.2%). Candidate.Shizhenmycota exhibited within-lineage sequence identities of 46.7–91.6% (coverage 77.2–99.3%), compared with only 45.2–55.4% identity and coverage (77.0–86.8%) to Zoopagomycota references. Similarly, Candidate.Xihemycota showed within-lineage identities of 49.1–93.0% (coverage 82.8–99.8%), whereas comparisons with Zoopagomycota references yielded only 50.2–59.1% identity and coverage (76.9–85.9%). Notably, pairwise comparisons between Candidate.Xihemycota and Candidate.Shizhenmycota showed identities ranging from 43.3% to 65.6% (coverage 72.9–93.3%), further supporting their distinction as separate lineages despite their close phylogenetic relationship. These phylogenetic and sequence

data collectively indicate that the three lineages are genetically distinct from their nearest recognized relatives and from each other. Therefore, these three lineages were tentatively referred to as Candidate.Taichumycota, Candidate.Shizhenmycota, and Candidate.Xihemycota pending additional genomic and morphological evidence.

Table 1. Sequence divergence within three candidate fungal lineages and between each lineage and its closest recognized relatives based on the amplified 28S rRNA sequences.

	Identity(%)	Coverage(%)
Within Candidate.Taichumycota	84.6–92.6	97.2–99.6
Within Candidate.Shizhenmycota	46.7–91.6	77.2–99.3
Within Candidate.Xihemycota	49.1–93.0	82.8–99.8
Between Candidate.Taichumycota and Aphelida	68.4–69.3	95.5–97.2
Between Candidate.Shizhenmycota and Zoopagomycota	45.2–55.4	77.0–86.8
Between Candidate.Xihemycota and Zoopagomycota	50.2–59.1	76.9–85.9
Between Candidate.Xihemycota and Candidate.Shizhenmycota	43.3–65.6	72.9–93.3

Note: The values shown represent pairwise sequence identity and alignment coverage calculated from 28S rRNA amplicon-region alignments. All comparisons were performed using trimmed sequences corresponding to the amplified region and therefore do not reflect variation outside the target amplicon region included in the phylogenetic analysis shown in Figure 3.

Taxonomic composition showed different patterns across water layers (Figure 2; Figure 4 – 5). Surface communities contained representatives from all 35 detected fungal phyla and were characterized by relatively high proportions of Ascomycota (63.1%), Basidiomycota (13.8%), and Chytridiomycota (6.2%). In contrast, mesopelagic and bathypelagic communities showed stronger dominance by Ascomycota, accounting for 92.3% and 83.5% of sequences, respectively. Sediment communities displayed a distinct taxonomic profile, with reduced relative abundance of Ascomycota (64.9%) and increased contributions from Basidiomycota (29.9%) and Chytridiomycota (4.3%). The three candidate deep-branching lineages also showed different vertical stratification (Figure 4). Candidate.Taichumycota was detected exclusively in surface waters. Candidate.Shizhenmycota was most abundant in surface communities but occurred at lower relative abundances throughout the water column, whereas Candidate.Xihemycota was detected across all water layers and reached its highest relative abundance in sediments. Similar compositional patterns were observed at the genus level (Figure 5; Additional file 9). Surface communities contained a large proportion of unassigned taxa (32.5%), together with abundant *Nectria* (27.5%), *Emmonsiellopsis* (14.7%), and *Penicillium* (6.7%). In mesopelagic communities, *Nectria* accounted for 77.5% of sequences and remained abundant in bathypelagic waters (56.0%). Bathypelagic communities also contained relatively high proportions of *Emmonsiellopsis* (13.5%) and *Malassezia* (10.7%). Sediment communities were dominated by *Emmonsiellopsis* (41.5%), followed by *Malassezia* (16.5%), *Nectria* (12.5%), and *Filobasidium* (11.2%).

Environmental and geographic factors shaping fungal community structure across the tropical Indian Ocean and western Pacific Ocean

Beta-diversity analyses based on Bray–Curtis dissimilarity revealed significant

differentiation of fungal community composition among water layers across the tropical Indian Ocean and western Pacific Ocean (Figure 6; Table 2; Table S1). PERMANOVA showed that water layer significantly influenced fungal community structure, explaining 12.4% of the total variation ($R^2 = 0.124$, $p = 0.001$). ANOSIM analysis also detected significant differences among water layers, although the separation strength was relatively modest ($R = 0.121$, $p = 0.018$). Together, these results indicate that vertical habitat differentiation represents an important factor associated with variation in marine fungal community composition, while substantial unexplained variation remained among samples. Pairwise comparisons further demonstrated significant differentiation among water-layer communities (Table S1). The strongest separation occurred between mesopelagic and sediment communities, followed by comparisons involving bathypelagic and sediment habitats, whereas surface communities showed comparatively weaker differentiation from other habitats. Principal coordinate analysis (PCoA) based on Bray–Curtis dissimilarity further supported the vertical differentiation pattern, with samples showing partial separation according to habitat type (Figure 6). The first and second PCoA axes explained 26.7% and 9.5% of total community variation, respectively, although considerable overlap remained among water layers.

Table 2. Analysis of dissimilarity in fungal communities across different water layers in the tropical Indian Ocean and western Pacific Ocean using ANOSIM and PERMANOVA.

ANOSIM Analysis		
Variable	R-Value	*P*-Value
Layer	0.121175	**0.018**
PERMANOVA (adonis) Analysis		

Variable	R^2	*P*-Value
Layer	0.124389	**0.001**

Note: Analyses were based on Bray-Curtis dissimilarity. For ANOSIM, R > 0 indicates greater dissimilarity between groups than within groups. For PERMANOVA, R^2 represents the proportion of variance explained. *P*-value < 0.05 is considered statistically significant and is shown in bold.

Table S1. Pairwise PERMANOVA (Adonis) analysis of fungal community dissimilarity across different water layers in the tropical Indian Ocean and western Pacific Ocean.

PERMANOVA (adonis) Analysis		
Factor	R^2	*P*-Value
Surface and Mesopelagic	0.093	**0.001**
Surface and Bathypelagic	0.032	**0.002**
Surface and Sediment	0.023	**0.009**
Mesopelagic and Bathypelagic	0.156	**0.014**
Mesopelagic and Sediment	0.598	**0.002**
Bathypelagic and Sediment	0.228	**0.033**

Note: Pairwise PERMANOVA (Adonis) was performed based on Bray–Curtis dissimilarity. R^2 represents the proportion of variance explained. *P*-value < 0.05 is considered statistically significant and is shown in bold.

Because sampling effort was strongly uneven among water layers, environmental and geographic analyses were restricted to surface communities to minimize biases

associated with unequal sample sizes. Geographic and environmental variables exhibited distinct relationships with fungal alpha diversity patterns in surface waters of the tropical Indian and western Pacific Oceans (Additional file 10). Among geographic factors, longitude exhibited significant relationships with multiple diversity indices. Longitude was positively associated with observed richness but negatively associated with Shannon diversity, Simpson diversity, and Pielou's evenness (Figure 7). In contrast, latitude showed no significant associations with any alpha diversity metric ($p > 0.05$). Among environmental variables, salinity and phosphate concentration were significantly associated with fungal diversity patterns, whereas SST, chlorophyll *a*, and nitrate showed no significant relationships with alpha diversity indices. Both salinity and phosphate displayed similar trends, with higher values associated with increased observed richness but reduced Shannon diversity, Simpson diversity, and community evenness. Among all variables examined, phosphate showed the strongest associations with alpha diversity variation, particularly for community evenness (Figures 7–8).

To further evaluate the relative contributions of geographic and environmental factors to fungal community composition, redundancy analysis (RDA) was performed using surface fungal communities (Figure 9). The overall RDA model was significant ($F = 2.644$, $p = 0.001$) and explained 18.6% of the total variation in fungal community composition. Partial RDA demonstrated significant contributions from both geographic and environmental components, with environmental variables ($F = 1.922$, $p = 0.001$) and geographic variables ($F = 3.085$, $p = 0.001$) each contributing significantly to community variation. Variation partitioning revealed that pure environmental effects and pure geographic effects independently explained 4.7% and 4.4% of community variation, respectively, while their shared contribution accounted for an additional 2.4%. Marginal effects analysis identified longitude as the strongest individual predictor,

explaining 5.52% of the variation in fungal community composition, followed by phosphate concentration (4.73%) and salinity (3.39%) (Table 3). These results indicate that large-scale geographic gradients and environmental heterogeneity jointly contribute to shaping surface fungal community composition in the tropical Indian Ocean and western Pacific Ocean.

Table 3. Marginal effects of geographic and environmental variables on surface fungal community composition based on redundancy analysis (RDA).

Explanatory variable	Explained variance (%)	F-Value	*P*-Value
Longitude	5.52	5.087	**0.001**
Phosphate	4.73	4.324	**0.001**
Salinity	3.39	3.052	**0.001**
Latitude	3.30	2.972	**0.001**
Nitrate	2.47	2.202	**0.001**
SST	2.22	1.971	**0.013**
Chlorophyll *a*	2.12	1.887	**0.001**

Note: Marginal effects were assessed using individual RDA models with each explanatory variable fitted separately. Explained variance (%) represents the adjusted proportion of fungal community variation explained by each predictor alone. F-values indicate the strength of predictor effects relative to residual variation. Variables are ranked according to their individual explanatory power. *P*-value < 0.05 is considered statistically significant and is shown in bold.

Prediction of fungal functional guilds

Beta diversity analyses of predicted fungal functional guild composition indicated significant variation among water layers (Table 4). PERMANOVA showed that water

layer explained 21.1% of the variation in predicted functional guild composition (R^2 = 0.211, p = 0.001). ANOSIM produced a consistent result, indicating significant differences in predicted functional guild composition among water layers (R = 0.178, p = 0.001).

FUNGuild predictions suggested that the relative composition of predicted fungal guilds varied across water layers (Figure 10, Additional file 11-12). Surface communities exhibited relatively high functional heterogeneity, with predicted functional assignments distributed among undefined taxa (17.2%), plant pathogens (11.0%), wood saprotrophs (10.6%), endophytes (10.5%), fungal parasites (9.8%), undefined saprotrophs (9.9%), animal pathogens (9.2%), and plant saprotrophs (8.4%). Predicted functional guild compositions in the mesopelagic and bathypelagic layers were broadly similar, with relatively even contributions from pathogenic, parasitic, endophytic, and saprotrophic guilds, each accounting for approximately 12–14% of the total predicted functional assignments. In contrast, sediment communities showed a distinct predicted functional guild composition, with a markedly higher relative abundance of undefined saprotrophs (35.1%) and comparatively lower proportions of predicted endophytes, plant pathogens, and wood saprotrophs than those observed in pelagic communities.

Table 4. ANOSIM and PERMANOVA (Adonis) analyses of predicted fungal functional guild composition across different water layers in the tropical Indian Ocean and western Pacific Ocean based on Bray–Curtis dissimilarity.

ANOSIM Analysis		
Factor	R-value	*P*-value
Layers	0.178	**0.001**

PERMANOVA (Adonis) Analysis

Factor	R^2	*P*-Value
Layers	0.211	**0.001**

Note: Analyses were based on Bray–Curtis dissimilarity of predicted fungal functional guild composition inferred using FUNGuild. For ANOSIM, R-value > 0 indicate greater dissimilarity between groups than within groups. For PERMANOVA (Adonis), R^2 represents the proportion of variance explained. $P < 0.05$ was considered statistically significant and is shown in bold.

Discussion

This study provides a comprehensive assessment of fungal diversity across the tropical Indian Ocean and western Pacific Ocean using long-read 28S rRNA metabarcoding. A total of 46,938 fungal OTUs were recovered from 113 samples, representing 35 phyla, 164 classes, 254 orders, 509 families, 940 genera, and 1,055 species, highlighting the extensive diversity of the marine mycobiome. At the phylum level, fungal communities were primarily dominated by Ascomycota (67.47%) and Basidiomycota (13.43%). Although Ascomycota and Basidiomycota dominated marine fungal communities, consistent with previous surveys of coastal and benthic environments [48–50], our results further demonstrated substantial contributions from early-diverging fungal lineages [48], including Chytridiomycota (5.18%) and Rozellomycota (2.35%). The widespread occurrence of Chytridiomycota across marine habitats is consistent with their recognized ecological roles in planktonic ecosystems, where parasitic interactions with phytoplankton may facilitate carbon transfer through the aquatic mycoloop pathway [49]. In contrast, many members of Rozellomycota remain poorly characterized due to limited cultivation and functional information, despite their

frequent detection in aquatic environments [50]. The detection of additional low-abundance lineages, including Mucoromycota (2.14%), Mortierellomycota (0.65%), Olpidiomycota (0.33%), Aphelidiomycota (0.09%), and Monoblepharomycota (0.83%), further highlights that marine fungal diversity extends well beyond the traditionally recognized dominant groups [51].

At the genus level, *Nectria* was the overwhelmingly dominant genus in our dataset, accounting for 33.89% of the total fungal abundance, followed by *Emmonsiellopsis* (14.92%), *Penicillium* (5.41%), and *Malassezia* (4.95%). However, a considerable proportion of sequences (27.70%) could not be assigned to described genera, emphasizing the large proportion of unresolved fungal diversity in tropical oceanic ecosystems [52, 53]. The predominance of *Nectria* in our dataset is noteworthy, as this genus has been frequently detected in marine environments, particularly in association with coral-associated communities and deep-sea sediments [54, 55]. Members of *Nectria* are known to exhibit diverse ecological strategies, including saprotrophic decomposition of organic matter and potential pathogenic interactions with marine organisms [56]. The high relative abundance of *Emmonsiellopsis* in our study is consistent with previous observations in marine sediments and coral-associated environments, where this genus has been reported as a common component of benthic fungal communities[18, 23]. *Penicillium*, though ranking third in overall abundance, has been widely reported as a dominant genus in various marine habitats, including mangrove sediments, marine sponges, and polar environments [57, 58]. The repeated detection of *Penicillium* across diverse marine environments may reflect its broad environmental tolerance and capacity to colonize various marine substrates [59]. Previous studies have suggested that *Penicillium* species can function as marine-associated saprotrophs involved in organic matter decomposition and nutrient recycling,

while also producing diverse secondary metabolites with potential effects on microbial interactions [60, 61]. *Malassezia*, a genus primarily known as a mammalian skin commensal and pathogen, has been increasingly recognized as a widespread component of marine fungal communities, particularly in pelagic environments [16]. Its presence in our dataset across multiple water layers suggests that this genus may play previously unrecognized ecological roles in marine ecosystems.

Importantly, the high proportion of unresolved taxa observed in this study indicates that current assessments likely underestimate marine fungal diversity. Instead of excluding unclassified sequences [62, 63], phylogenetic analyses of deeply divergent OTUs revealed three independent lineages that could not be assigned to currently recognized fungal phyla. Candidate.Taichumycota formed a lineage sister to Aphelida, whereas Candidate.Shizhenmycota and Candidate.Xihemycota formed a divergent lineage associated with Zoopagomycota. Their distinct phylogenetic positions and low sequence similarity to recognized groups support their status as deeply divergent candidate lineages, although further morphological observations and multi-locus phylogenomic analyses are required for formal taxonomic evaluation. The discovery of these candidate lineages suggests that marine ecosystems represent important reservoirs of previously unrecognized fungal evolutionary diversity [46]. The high fungal diversity detected in this study likely reflects several methodological improvements. First, the application of long-read 28S rRNA metabarcoding provided longer phylogenetic information compared with conventional short-read approaches, facilitating improved resolution of divergent fungal lineages [61, 64]. Second, the integration of multiple reference databases, including SILVA [65], the NCBI BLAST nucleotide database (https://ftp.ncbi.nlm.nih.gov/blast/db/), and EUKARYOME [66], expanded the available sequence framework and may have improved taxonomic

assignment [61, 64]. Third, subsequent phylogenetic placement of initially unclassified OTUs enabled the recognition of deeply divergent fungal lineages that would otherwise remain unresolved as environmental sequences. Together, these approaches enhanced the detection and characterization of previously overlooked marine fungal diversity. Nevertheless, several limitations should be considered. Although a 97% sequence similarity threshold was adopted in this study based on previous fungal LSU studies [67] and to facilitate comparisons with existing datasets, OTU-based clustering may underestimate fine-scale sequence variation among closely related fungal taxa. Future investigations integrating ASV-based approaches, multiple molecular markers, and expanded marine fungal genome resources will further improve the resolution of marine fungal diversity assessments [35].

Fungal communities exhibited pronounced vertical stratification across the tropical Indian Ocean and western Pacific Ocean. PERMANOVA and ANOSIM analyses based on Bray–Curtis dissimilarity demonstrated significant differentiation among water layers, although water depth explained only a moderate proportion of total community variation ($R^2 = 0.124$). The strongest differentiation occurred between mesopelagic and sediment communities, suggesting that depth-related habitat transitions represent important ecological gradients shaping marine fungal assemblages. Similar depth-associated differentiation has been reported in global marine fungal surveys, where planktonic and benthic fungal communities exhibited distinct assemblage structures, with only 15.4% of OTUs shared between water-column and sediment habitats, highlighting strong ecological differentiation between pelagic and benthic environments [4]. Such habitat-associated community differentiation may reflect differences in resource availability, substrate characteristics, and organic matter sources among marine environments [18, 25, 68]. Sediment environments provide abundant

particulate organic substrates and frequently harbor saprotrophic fungal taxa involved in organic matter degradation, whereas pelagic fungal communities experience contrasting resource regimes and particle-associated habitats [18, 25, 68]. Therefore, vertical patterns of marine fungal communities may not simply represent responses to depth gradients, but rather reflect the combined effects of habitat transitions, environmental filtering, and ecological specialization across contrasting marine environments.

Because sampling effort was strongly uneven among water layers, environmental and geographic analyses were restricted to surface communities to minimize biases associated with unequal sample sizes. The RDA model explained 18.6% of the variation in fungal community composition, with significant contributions from both geographic and environmental variables. Variation partitioning further showed comparable independent effects of geographic factors (4.4%) and environmental factors (4.7%), together with shared contributions (2.4%), indicating that surface fungal communities are jointly structured by spatial gradients and environmental heterogeneity.

Among geographic variables, longitude emerged as the strongest predictor of fungal community composition, explaining 5.52% of total variation in the RDA model. Longitude was also significantly associated with all alpha diversity metrics, showing a positive relationship with observed richness but negative relationships with Shannon diversity, Simpson diversity, and Pielou's evenness. This pattern suggests that longitudinal gradients may influence not only fungal richness but also community organization by altering the relative dominance of different taxa. Similar spatial patterns have been reported in marine fungal communities from the Gulf of Mexico, where both latitude and longitude contributed to the distribution patterns of marine ascomycete communities [25]. At large spatial scales, longitudinal variation may integrate multiple

oceanographic processes, including differences in ocean circulation, water mass characteristics, and regional environmental heterogeneity [4]. In the tropical Indian Ocean and western Pacific Ocean, extensive connectivity among oceanic regions may facilitate the dispersal of fungal propagules, whereas regional differences in hydrographic conditions may influence local establishment and dominance patterns [69, 70]. Unlike longitude, latitude showed no significant relationships with alpha diversity metrics in this study, although it contributed significantly to variation in community composition. This indicates that latitudinal gradients may influence species turnover and community assembly processes rather than local diversity levels. Similar weak relationships between latitude and marine fungal diversity have been reported in global surveys, suggesting that classical latitudinal diversity gradients may not universally apply to marine fungi [16, 71]. The high dispersal potential of fungal propagules, particle-mediated transport, and oceanic connectivity may weaken the influence of geographic distance and contribute to the absence of clear latitudinal diversity patterns [16, 70]. However, the relative roles of dispersal processes and environmental filtering in shaping marine fungal biogeography remain unresolved and require further investigation using broader spatial sampling and long-term observations [16].

Among environmental variables, phosphate availability emerged as one of the most important factors associated with fungal diversity and community composition. Phosphate showed a positive relationship with observed richness but negative relationships with Shannon diversity, Simpson diversity, and Pielou's evenness. Consistently, phosphate explained the largest proportion of variation among alpha diversity metrics and accounted for 4.73% of community variation in the RDA analysis. These patterns suggest that phosphate availability may enhance the recruitment or persistence of additional fungal taxa while simultaneously increasing the dominance of

competitive or opportunistic groups. Similar nutrient-associated shifts have been observed in coastal sediments and marginal seas, where phosphorus availability influences fungal assemblage structure and ecological interactions [18, 23]. For example, nutrient enrichment in coastal sediments has been shown to increase fungal richness while promoting dominance by opportunistic taxa, resulting in reduced community evenness [23]. Furthermore, phosphorus availability has been identified as an important factor regulating marine sediment fungal communities, with phosphate concentrations significantly associated with the abundance of dominant fungal phyla such as Ascomycota and Basidiomycota [18]. Salinity also exhibited significant effects on fungal diversity and community composition, explaining 3.39% of community variation in the RDA model. Salinity was positively correlated with observed richness but negatively correlated with Shannon diversity, Simpson diversity, and Pielou's evenness. Similar salinity-associated structuring of marine fungal communities has been reported across diverse environments. For example, Baltic Sea studies demonstrated that salinity was a major predictor of benthic fungal community composition, with distinct assemblages occurring along salinity gradients [72]. Similarly, coastal sediment studies from Guangdong, China, showed that salinity significantly influenced fungal diversity, with differences in richness between low- and high-salinity environments [18]. In contrast to salinity and phosphate, temperature, chlorophyll a, and nitrate showed limited relationships with fungal alpha diversity, although they contributed significantly to community composition in the RDA model. This discrepancy suggests that these variables may primarily influence community structure and taxonomic composition rather than overall diversity patterns. Chlorophyll a and nitrate may affect marine fungal assemblages indirectly by regulating phytoplankton productivity, organic carbon availability, and particle-associated habitats,

thereby altering resource conditions and competitive interactions among fungal taxa rather than directly determining fungal richness [73, 74]. Consistent with this interpretation, previous studies have shown that nitrate availability can significantly influence marine fungal community composition, with changes in dissolved inorganic nitrogen associated with shifts in fungal assemblage structure [4, 75]. The relatively weak association between temperature and alpha diversity suggests that thermal gradients may play a limited role in shaping local diversity patterns of marine fungal communities in the tropical Indian Ocean and western Pacific Ocean, compared with other environmental factors such as nutrient availability [4, 16].

Predicted functional guild composition exhibited significant vertical differentiation across the tropical Indian Ocean and western Pacific Ocean. Functional beta-diversity analysis showed that water layer explained 21.1% of the variation in predicted functional composition ($R^2 = 0.211$, $p = 0.001$). Surface communities exhibited the highest functional heterogeneity, with predicted assignments distributed among multiple ecological guilds, including plant pathogens, wood saprotrophs, endophytes, fungal parasites, and undefined saprotrophs. This pattern is consistent with previous studies showing that planktonic marine fungi encompass diverse trophic modes [69, 70]. The high functional diversity of surface communities may be associated with heterogeneous organic substrates derived from primary production, phytoplankton mortality, terrestrial inputs, and sinking particles, which collectively generate diverse ecological niches supporting the coexistence of fungi with contrasting ecological strategies [73, 76]. In contrast, mesopelagic and bathypelagic communities exhibited relatively similar predicted functional profiles. This similarity may be associated with vertical ecological connectivity mediated by sinking particulate organic matter. Marine snow links surface and deep ocean environments by transporting organic carbon and

595 microbial biomass into the deep ocean, thereby providing nutritional resources and
596 microscale habitats for heterotrophic microorganisms, including fungi [70, 73].
597 Sediment communities displayed distinct functional characteristics compared with
598 pelagic habitats, primarily characterized by a strong enrichment of undefined
599 saprotrophs (35.1%). This pattern is consistent with previous studies showing that
600 marine sediments generally harbor abundant saprotrophic fungi involved in organic
601 matter degradation and carbon transformation processes [77]. However, these
602 functional assignments remain predictive because FUNGuild is mainly based on well-
603 characterized terrestrial fungi, while many marine fungal lineages remain poorly
604 represented in current databases [45, 70]. Therefore, future integration of metagenomics,
605 metatranscriptomics, metabolomics, and cultivation-based approaches will be
606 necessary to further validate the ecological functions of marine fungi.

607 **Conclusions**

608 Marine fungi represent an important yet still poorly characterized component of ocean
609 ecosystems. Using long-read 28S rRNA metabarcoding across the tropical Indian
610 Ocean and western Pacific Ocean, this study revealed extensive fungal diversity,
611 including a large proportion of unresolved sequences and three deeply divergent
612 candidate fungal lineages. These findings suggest that current assessments based on
613 available reference resources likely underestimate the evolutionary diversity of marine
614 fungi. Fungal communities exhibited significant vertical differentiation across surface
615 waters, mesopelagic and bathypelagic zones, and sediments, although water layer
616 explained only a moderate proportion of community variation. Surface fungal
617 community composition was jointly associated with geographic gradients and
618 environmental variability, with longitude, phosphate, and salinity emerging as
619 important predictors. Predicted ecological guild composition exhibited clear vertical

differentiation, with sediment environments particularly enriched in predicted undefined saprotrophic guilds, potentially reflecting the distinct organic matter regimes and ecological conditions of benthic habitats. Together, this study expands our understanding of marine fungal diversity and biogeographic patterns in the tropical Indian and western Pacific Oceans, revealing previously unrecognized evolutionary lineages and complex environmental associations. Future investigations integrating multi-locus phylogenomics, cultivation approaches, metatranscriptomics, and expanded environmental sampling will be essential for resolving the ecological functions and evolutionary origins of these newly identified fungal lineages.

Declarations

Ethics approval and consent to participate

Not applicable.

Consent for publication

Not applicable.

Availability of data and materials

The analysis code and scripts for data processing are provided in Additional file 4. Environmental measurements collected at the time of sampling are presented in Additional files 1-2. The raw sequencing data of fungi from 113 samples have been deposited in the NCBI Sequence Read Archive (SRA) under BioProject accession PRJNA1462484 (https://identifiers.org/bioproject:PRJNA1462484). To allow access during peer review, the data can be viewed via the following reviewer link: https://dataview.ncbi.nlm.nih.gov/object/PRJNA1462484?reviewer=e7g3pi19dka7e5g3nij36njb2t. The predicted functional guild composition of the fungal communities is available in Additional file 11.

Competing interests

The authors declare that they have no competing interests.

Funding

This work was supported by the Guangxi Science and Technology Program (No. AD25069075), the National Natural Science Foundation of China (42030502), the Central Public-Interest Scientific Institution Basal Research Fund (PM-zx703-202506-180, PM-zx703-202506-206, PM-zx703-202408-288).

Authors' contributions

All authors contribute to the preparation of the previous and revised manuscript, which can be seen as follows: Sanqiang Gong: Conceptualization, Investigation, Sampling, Methodology, Writing-review and editing. Kefu Yu, Resources, Writing-review and editing and Funding acquisition. Leilei Huang, formal analysis, Writing-original draft. Lijia Xu, Resources, Writing-review and editing. Honglei, Jiang, data collection. Guangjun Chai and Yuxiao Li, Writing-review and editing.

Acknowledgements

Not applicable.

References

1. Bar-On YM, Phillips R, Milo R. The biomass distribution on Earth. Proc Natl Acad Sci USA. 2018;115:6506–11. https://doi.org/10.1073/pnas.1711842115.
2. Cavicchioli R, Ripple WJ, Timmis KN, Azam F, Bakken LR, Baylis M, et al. Scientists' warning to humanity: microorganisms and climate change. Nat Rev Microbiol. 2019;17:569–86. https://doi.org/10.1038/s41579-019-0222-5.
3. Breyer E, Stix C, Kilker S, Roller BRK, Panagou F, Doebke C, et al. The contribution of pelagic fungi to ocean biomass. Cell. 2025;188:3992-4002.e13. https://doi.org/10.1016/j.cell.2025.05.004.
4. Tisthammer KH, Cobian GM, Amend AS. Global biogeography of marine fungi is shaped by the environment. Fungal Ecology. 2016;19:39–46. https://doi.org/10.1016/j.funeco.2015.09.003.
5. Zinger L, Amaral-Zettler LA, Fuhrman JA, Horner-Devine MC, Huse SM, Welch DBM, et al. Global Patterns of Bacterial Beta-Diversity in Seafloor and Seawater Ecosystems. PLoS ONE. 2011;6:e24570. https://doi.org/10.1371/journal.pone.0024570.

6. Vitanza L, Coccia AM, Peluso A, Brandtner D, Muratore A, Ferrara F, et al. Global mapping and environmental drivers of epipelagic bacterial communities in the open oceans. Front Mar Sci. 2025;12:1625011. https://doi.org/10.3389/fmars.2025.1625011.
7. Zhang X, Zhang C, Liu Y, Zhang R, Li M. Non-negligible roles of archaea in coastal carbon biogeochemical cycling. Trends in Microbiology. 2023;31:586–600. https://doi.org/10.1016/j.tim.2022.11.008.
8. Morales SE, Holben WE. Linking bacterial identities and ecosystem processes: can 'omic' analyses be more than the sum of their parts?: Toward linking bacterial identities and ecosystem processes. FEMS Microbiology Ecology. 2011;75:2–16. https://doi.org/10.1111/j.1574-6941.2010.00938.x.
9. Zinger L, Boetius A, Ramette A. Bacterial taxa–area and distance–decay relationships in marine environments. Molecular Ecology. 2014;23:954–64. https://doi.org/10.1111/mec.12640.
10. Zhang C-J, Chen Y-L, Sun Y-H, Pan J, Cai M-W, Li M. Diversity, metabolism and cultivation of archaea in mangrove ecosystems. Mar Life Sci Technol. 2021;3:252–62. https://doi.org/10.1007/s42995-020-00081-9.
11. Amend AS, Oliver TA, Amaral-Zettler LA, Boetius A, Fuhrman JA, Horner-Devine MC, et al. Macroecological patterns of marine bacteria on a global scale. Journal of Biogeography. 2013;40:800–11. https://doi.org/10.1111/jbi.12034.
12. Asseri AA, Coello-Camba A, Agustí S. Fungal planktonic community related to salinity and temperature in an oligotrophic sea. Front Microbiol. 2025;16:1435925. https://doi.org/10.3389/fmicb.2025.1435925.
13. Hawksworth DL, Lücking R. Fungal Diversity Revisited: 2.2 to 3.8 Million Species. Microbiol Spectr. 2017;5:5.4.10. https://doi.org/10.1128/microbiolspec.FUNK-0052-2016.
14. Debeljak P, Baltar F. Fungal Diversity and Community Composition across Ecosystems. Journal of Fungi. 2023;9:510. https://doi.org/10.3390/jof9050510.
15. Zhao H, Brearley FQ, Huang L, Tang J, Xu Q, Li X, et al. Abundant and Rare Taxa of Planktonic Fungal Community Exhibit Distinct Assembly Patterns Along Coastal Eutrophication Gradient. Microb Ecol. 2023;85:495–507. https://doi.org/10.1007/s00248-022-01976-z.
16. Hassett BT, Vonnahme TR, Peng X, Jones EBG, Heuzé C. Global diversity and geography of planktonic marine fungi. Botanica Marina. 2020;63:121–39. https://doi.org/10.1515/bot-2018-0113.
17. Chen J, McIlroy SE, Archana A, Baker DM, Panagiotou G. A pollution gradient contributes to the taxonomic, functional, and resistome diversity of microbial communities in marine sediments. Microbiome. 2019;7:104. https://doi.org/10.1186/s40168-019-0714-6.
18. Wu K, Liu Y, Liao X, Yang X, Chen Z, Mo L, et al. Fungal Diversity and Its Relationship with Environmental Factors in Coastal Sediments from Guangdong, China. Journal of Fungi. 2023;9:101. https://doi.org/10.3390/jof9010101.
19. Dang Q, Wang Y, Xiong S, Yu H, Zhao X, Tan W, et al. Untangling the response of fungal community structure, composition and function in soil aggregate fractions to food waste compost addition. Science of The Total Environment. 2021;769:145248.

https://doi.org/10.1016/j.scitotenv.2021.145248.
20. Falkowski PG, Fenchel T, Delong EF. The Microbial Engines That Drive Earth's Biogeochemical Cycles. Science. 2008;320:1034–9. https://doi.org/10.1126/science.1153213.
21. Varrella S, Barone G, Corinaldesi C, Giorgetti A, Nomaki H, Nunoura T, et al. Fungal Abundance and Diversity in the Mariana Trench, the Deepest Ecosystem on Earth. JoF. 2024;10:73. https://doi.org/10.3390/jof10010073.
22. Li W, Wang MM, Wang XG, Cheng XL, Guo JJ, Bian XM, et al. Fungal communities in sediments of subtropical Chinese seas as estimated by DNA metabarcoding. Sci Rep. 2016;6:26528. https://doi.org/10.1038/srep26528.
23. Gao M, Liu B, Li J, Deng Y, Zhang Y, Zhang N, et al. Diversity and Distribution of Fungi in the Marine Sediments of Zhanjiang Bay, China. Journal of Fungi. 2024;10:867. https://doi.org/10.3390/jof10120867.
24. Lobo LQ, Izabel-Shen D, Albertsson J, Raymond C, Gunnarsson JS, Broman E, et al. Salinity and resource availability as drivers of Baltic benthic fungal diversity. Environmental DNA. 2024;6:e526. https://doi.org/10.1002/edn3.526.
25. Walker AK, Robicheau BM. Fungal diversity and community structure from coastal and barrier island beaches in the United States Gulf of Mexico. Sci Rep. 2021;11:3889. https://doi.org/10.1038/s41598-021-81688-5.
26. Tian J, Zhu D, Wang J, Wu B, Hussain M, Liu X. Environmental factors driving fungal distribution in freshwater lake sediments across the Headwater Region of the Yellow River, China. Sci Rep. 2018;8:3768. https://doi.org/10.1038/s41598-018-21995-6.
27. Ambati M, Kumar MS. Microbial Diversity in the Indian Ocean Sediments: An Insight into the Distribution and Associated Factors. Curr Microbiol. 2022;79:115. https://doi.org/10.1007/s00284-022-02801-z.
28. Ding C, Wu C, Guo C, Gui J, Wei Y, Sun J. The Composition and Primary Metabolic Potential of Microbial Communities Inhabiting the Surface Water in the Equatorial Eastern Indian Ocean. Biology. 2021;10:248. https://doi.org/10.3390/biology10030248.
29. Burris JE, Porter JW, Laing WA. Effects of carbon dioxide concentration on coral photosynthesis. Mar Biol. 1983;75:113–6. https://doi.org/10.1007/BF00405992.
30. Price N, Hamilton S, Tootell J, Smith J. Species-specific consequences of ocean acidification for the calcareous tropical green algae Halimeda. Mar Ecol Prog Ser. 2011;440:67–78. https://doi.org/10.3354/meps09309.
31. Assis J, Tyberghein L, Bosch S, Verbruggen H, Serrão EA, De Clerck O. Bio-ORACLE v2.0: Extending marine data layers for bioclimatic modelling. Global Ecology and Biogeography. 2018;27:277–84. https://doi.org/10.1111/geb.12693.
32. Tedersoo L, Jairus T, Horton BM, Abarenkov K, Suvi T, Saar I, et al. Strong host preference of ectomycorrhizal fungi in a Tasmanian wet sclerophyll forest as revealed by DNA barcoding and taxon-specific primers. New Phytologist. 2008;180:479–90. https://doi.org/10.1111/j.1469-8137.2008.02561.x.
33. Bolyen E, Rideout JR, Dillon MR, Bokulich NA, Abnet CC, Al-Ghalith GA, et al. Reproducible, interactive, scalable and extensible microbiome data science using QIIME 2. Nat Biotechnol. 2019;37:852–7. https://doi.org/10.1038/s41587-019-0209-9.

764 34. Martin M. Cutadapt removes adapter sequences from high-throughput sequencing
765 reads. EMBnet.journal. 2011;17:10–2. https://doi.org/10.14806/ej.17.1.200.
766 35. Callahan BJ, McMurdie PJ, Rosen MJ, Han AW, Johnson AJA, Holmes SP. DADA2:
767 High-resolution sample inference from Illumina amplicon data. Nat Methods.
768 2016;13:581–3. https://doi.org/10.1038/nmeth.3869.
769 36. Rognes T, Flouri T, Nichols B, Quince C, Mahé F. VSEARCH: a versatile open
770 source tool for metagenomics. PeerJ. 2016;4:e2584. https://doi.org/10.7717/peerj.2584.
771 37. Altschul SF, Gish W, Miller W, Myers EW, Lipman DJ. Basic local alignment search
772 tool. Journal of Molecular Biology. 1990;215:403–10. https://doi.org/10.1016/S0022-
773 2836(05)80360-2.
774 38. Katoh K, Standley DM. MAFFT Multiple Sequence Alignment Software Version 7:
775 Improvements in Performance and Usability. Mol Biol Evol. 2013;30:772–80.
776 https://doi.org/10.1093/molbev/mst010.
777 39. Minh BQ, Schmidt HA, Chernomor O, Schrempf D, Woodhams MD, von Haeseler
778 A, et al. IQ-TREE 2: New Models and Efficient Methods for Phylogenetic Inference in
779 the Genomic Era. Mol Biol Evol. 2020;37:1530–4.
780 https://doi.org/10.1093/molbev/msaa015.
781 40. Ronquist F, Teslenko M, van der Mark P, Ayres DL, Darling A, Höhna S, et al.
782 MrBayes 3.2: Efficient Bayesian Phylogenetic Inference and Model Choice Across a
783 Large Model Space. Syst Biol. 2012;61:539–42. https://doi.org/10.1093/sysbio/sys029.
784 41. McMurdie PJ, Holmes S. Shiny-phyloseq: Web application for interactive
785 microbiome analysis with provenance tracking. Bioinformatics. 2015;31:282–3.
786 https://doi.org/10.1093/bioinformatics/btu616.
787 42. Higdon R. Generalized Additive Models. In: Encyclopedia of Systems Biology.
788 Springer, New York, NY; 2013. p. 814–5. https://doi.org/10.1007/978-1-4419-9863-
789 7_1197.
790 43. Zuur AF, Ieno EN, Walker N, Saveliev AA, Smith GM. Mixed effects models and
791 extensions in ecology with R. New York, NY: Springer; 2009.
792 https://doi.org/10.1007/978-0-387-87458-6.
793 44. Borcard D, Gillet F, Legendre P. Numerical Ecology with R. Cham: Springer
794 International Publishing; 2018. https://doi.org/10.1007/978-3-319-71404-2.
795 45. Nguyen NH, Song Z, Bates ST, Branco S, Tedersoo L, Menke J, et al. FUNGuild:
796 An open annotation tool for parsing fungal community datasets by ecological guild.
797 Fungal Ecology. 2016;20:241–8. https://doi.org/10.1016/j.funeco.2015.06.006.
798 46. Pang K-L, Jones EBG, Abdel-Wahab MA, Adams SJ, Alves A, Azevedo E, et al.
799 Recent progress in marine mycological research in different countries, and prospects
800 for future developments worldwide. Botanica Marina. 2023;66:239–69.
801 https://doi.org/10.1515/bot-2023-0015.
802 47. González MC, González MC, Hanlin RT, Ulloa M. A checklist of higher marine
803 fungi of Mexico. Mycotaxon. 2001;80:241--253. https://doi.org/10.5962/p.418238.
804 48. Richards TA, Leonard G, Mahé F, del Campo J, Romac S, Jones MDM, et al.
805 Molecular diversity and distribution of marine fungi across 130 European
806 environmental samples. Proc R Soc B. 2015;282:20152243.
807 https://doi.org/10.1098/rspb.2015.2243.

808 49. Kagami M, Miki T, Takimoto G. Mycoloop: chytrids in aquatic food webs. Front
809 Microbiol. 2014;5. https://doi.org/10.3389/fmicb.2014.00166.
810 50. Jones MDM, Forn I, Gadelha C, Egan MJ, Bass D, Massana R, et al. Discovery of
811 novel intermediate forms redefines the fungal tree of life. Nature. 2011;474:200–3.
812 https://doi.org/10.1038/nature09984.
813 51. Tedersoo L, Bahram M, Põlme S, Kõljalg U, Yorou NS, Wijesundera R, et al. Global
814 diversity and geography of soil fungi. Science. 2014;346:1256688.
815 https://doi.org/10.1126/science.1256688.
816 52. Picard KT. Coastal marine habitats harbor novel early-diverging fungal diversity.
817 Fungal Ecology. 2017;25:1–13. https://doi.org/10.1016/j.funeco.2016.10.006.
818 53. Meyneng M, Tedersoo L, Burgaud G, Mikryukov V, Carriconde F, Lemonnier H, et
819 al. Diversity and Dispersal of Fungi Along a Subtropical Land-to-Sea Continuum.
820 Environ Microbiol Rep. 2026;18:e70297. https://doi.org/10.1111/1758-2229.70297.
821 54. Chen X, Liao X, Chang S, Chen Z, Yang Q, Peng J, et al. Comprehensive insights
822 into the differences of fungal communities at taxonomic and functional levels in stony
823 coral Acropora intermedia under a natural bleaching event. Marine Environmental
824 Research. 2024;196:106419. https://doi.org/10.1016/j.marenvres.2024.106419.
825 55. Dong W, Chen J, Liao X, Chen X, Huang L, Huang J, et al. Biodiversity,
826 Distribution and Functional Differences of Fungi in Four Species of Corals from the
827 South China Sea, Elucidated by High-Throughput Sequencing Technology. Journal of
828 Fungi. 2024;10:452. https://doi.org/10.3390/jof10070452.
829 56. Jones EBG, Pang K-L, Abdel-Wahab MA, Scholz B, Hyde KD, Boekhout T, et al.
830 An online resource for marine fungi. Fungal Diversity. 2019;96:347–433.
831 https://doi.org/10.1007/s13225-019-00426-5.
832 57. Cao G-P, Xia J-L, Zhao L-Y, Tang Z-Z, Lin X, Liu Y-H, et al. Penicixanthene E, a
833 new xanthene isolated from a mangrove-derived fungus Penicillium sp. J Antibiot.
834 2022;75:526–9. https://doi.org/10.1038/s41429-022-00548-0.
835 58. Liu C-C, Zhang Z-Z, Feng Y-Y, Gu Q-Q, Li D-H, Zhu T-J. Secondary metabolites
836 from Antarctic marine-derived fungus Penicillium crustosum HDN153086. Natural
837 Product Research. 2019;33:414–9. https://doi.org/10.1080/14786419.2018.1455045.
838 59. Osei SA, Dandi SO, Alhassan EH, Atindana SA. Marine Fungi in Coral Reefs:
839 Interactions and Ecological Significance. Marine Ecology. 2025;46:e70070.
840 https://doi.org/10.1111/maec.70070.
841 60. Abd El-Rahman TMA, Tharwat NA, Abo El-Souad SMS, El-Beih AA, El-Diwany
842 AI. Biological activities and variation of symbiotic fungi isolated from Coral reefs
843 collected from Red Sea in Egypt. Mycology. 2020;11:243–55.
844 https://doi.org/10.1080/21501203.2020.1741470.
845 61. Roik A, Reverter M, Pogoreutz C. A roadmap to understanding diversity and
846 function of coral reef-associated fungi. FEMS Microbiology Reviews. 2022;46:fuac028.
847 https://doi.org/10.1093/femsre/fuac028.
848 62. Góes-Neto A, Marcelino VR, Verbruggen H, Da Silva FF, Badotti F. Biodiversity
849 of endolithic fungi in coral skeletons and other reef substrates revealed with 18S rDNA
850 metabarcoding. Coral Reefs. 2020;39:229–38. https://doi.org/10.1007/s00338-019-
851 01880-y.

852 63. Rabbani G, Huang D, Wainwright BJ. The mycobiome of Pocillopora acuta in
853 Singapore. Coral Reefs. 2021;40:1419–27. https://doi.org/10.1007/s00338-021-02152-
854 4.
855 64. Frau A, Kenny JG, Lenzi L, Campbell BJ, Ijaz UZ, Duckworth CA, et al. DNA
856 extraction and amplicon production strategies deeply inf luence the outcome of gut
857 mycobiome studies. Sci Rep. 2019;9:9328. https://doi.org/10.1038/s41598-019-44974-
858 x.
859 65. Chuvochina M, Gerken J, Frentrup M, Sandikci Y, Goldmann R, Freese HM, et al.
860 SILVA in 2026: a global core biodata resource for rRNA within the DSMZ digital
861 diversity. Nucleic Acids Res. 2026;54:D334–41. https://doi.org/10.1093/nar/gkaf1247.
862 66. Tedersoo L, Hosseyni Moghaddam MS, Mikryukov V, Hakimzadeh A, Bahram M,
863 Nilsson RH, et al. EUKARYOME: the rRNA gene reference database for identification
864 of all eukaryotes. https://doi.org/10.1093/database/baae043.
865 67. Zhang ZF, Li M. Analysis of Fungal Community in Mangrove Sediments Based on
866 PacBio SMRT Sequencing. *BIO-PROTOCOL*. 2021.
867 https://doi.org/10.21769/BioProtoc.2003701.
868 68. Ogaki MB, Pinto OHB, Vieira R, Neto AA, Convey P, Carvalho-Silva M, et al.
869 Fungi Present in Antarctic Deep-Sea Sediments Assessed Using DNA Metabarcoding.
870 Microb Ecol. 2021;82:157–64. https://doi.org/10.1007/s00248-020-01658-8.
871 69. Hassett BT, Borrego EJ, Vonnahme TR, Rämä T, Kolomiets MV, Gradinger R.
872 Arctic marine fungi: biomass, functional genes, and putative ecological roles. ISME J.
873 2019;13:1484–96. https://doi.org/10.1038/s41396-019-0368-1.
874 70. Grossart H-P, Van den Wyngaert S, Kagami M, Wurzbacher C, Cunliffe M, Rojas-
875 Jimenez K. Fungi in aquatic ecosystems. Nat Rev Microbiol. 2019;17:339–54.
876 https://doi.org/10.1038/s41579-019-0175-8.
877 71. Morales SE, Biswas A, Herndl GJ, Baltar F. Global Structuring of Phylogenetic and
878 Functional Diversity of Pelagic Fungi by Depth and Temperature. Front Mar Sci.
879 2019;6. https://doi.org/10.3389/fmars.2019.00131.
880 72. Klawonn I, Van Den Wyngaert S, Parada AE, Arandia-Gorostidi N, Whitehouse MJ,
881 Grossart H-P, et al. Characterizing the “fungal shunt”: Parasitic fungi on diatoms affect
882 carbon flow and bacterial communities in aquatic microbial food webs. Proc Natl Acad
883 Sci USA. 2021;118:e2102225118. https://doi.org/10.1073/pnas.2102225118.
884 73. Chrismas N, Allen R, Allen MJ, Bird K, Cunliffe M. A 17-year time-series of fungal
885 environmental DNA from a coastal marine ecosystem reveals long-term seasonal-scale
886 and inter-annual diversity patterns. Proc R Soc B. 2023;290:20222129.
887 https://doi.org/10.1098/rspb.2022.2129.
888 74. Wang Y, Wang L, Liu Y, Su S, Hao W. Marine Bacterial Communities in the Xisha
889 Islands, South China Sea. Diversity. 2023;15:865. https://doi.org/10.3390/d15070865.
890 75. Xu W, Yang C, Luo Y, Zhang K, Chen M, Jiang S, et al. Distinct response of total
891 and active fungal communities and functions to seasonal changes in a semi-enclosed
892 bay with mariculture (DONGSHAN BAY , Southern CHINA). Limnology &
893 Oceanography. 2023;68:1048–63. https://doi.org/10.1002/lno.12328.
894 76. Wang H, Fang X, Wu H, Cai X, Xiao H. Effects of plant cultivars on the structure
895 of bacterial and fungal communities associated with ginseng. Plant Soil. 2021;465:143–

56. https://doi.org/10.1007/s11104-021-05000-0.
77. Li W, Wang M, Burgaud G, Yu H, Cai L. Fungal Community Composition and Potential Depth-Related Driving Factors Impacting Distribution Pattern and Trophic Modes from Epi- to Abyssopelagic Zones of the Western Pacific Ocean. Microb Ecol. 2019;78:820–31. https://doi.org/10.1007/s00248-019-01374-y.

Figure legends

Figure 1. Characterisation of environmental conditions and sampling sites across the tropical Indian and western Pacific Oceans. The map shows the spatial distribution of sampling sites and associated environmental gradients, including: (a) average sea surface temperature (SST, °C); (b) average sea surface salinity (PSU); (c) average chlorophyll *a* concentration (Chl *a*, $mg \cdot m^{-3}$); (d) average nitrate concentration ($\mu mol \cdot L^{-1}$); and (e) average phosphate concentration ($\mu mol \cdot L^{-1}$). Sampling sites are color-coded and shaped according to water depth: yellow circles, surface; green triangles, mesopelagic; blue triangles, bathypelagic; and red squares, sediment.

Figure 2. Phylum-level distribution of fungal communities across water layers in the tropical Indian and western Pacific Oceans. Panels show relative abundance at the phylum level for: (a) surface, (b) mesopelagic, (c) bathypelagic, and (d) sediment samples.

Figure 3. Phylogenetic analysis of 28S rRNA sequences from OTUs assigned to unclassified fungi. Representative 28S rRNA sequences from eleven recognized fungal phyla were included, with Stramenopiles sequences used as the outgroup. The scale bar represents 0.5 substitutions per site. Branch support values are shown as Bayesian posterior probabilities / SH-aLRT / ultrafast bootstrap values.

Figure 4. Distribution of novel candidate fungal phyla across water layers (heatmap). The horizontal axis represents (1) Candidate.Shizhenmycota, (2) Candidate.Taichumycota, and (3) Candidate.Xihemycota.

Figure 5. Distribution of the top 30 fungal genera across water layers in the tropical Indian Ocean and western Pacific Ocean. Panels show relative abundance for: (a) surface, (b) mesopelagic, (c) bathypelagic, and (d) sediment samples.

Figure 6. Principal coordinate analysis (PCoA) of fungal communities across the tropical Indian Ocean and western Pacific Ocean based on Bray–Curtis dissimilarity. Samples color-coded by water layer, with ellipses representing 95% confidence intervals. PCoA1 and PCoA2 axes explain 26.7% and 9.5% of the community variance, respectively. Statistical results were obtained from PERMANOVA analyses based on Bray–Curtis dissimilarity, where R^2 represents the proportion of explained variation and $p < 0.05$ indicates significant differences in community composition.

Figure 7. Observed OTU richness of surface fungal communities in relation to geographic (longitude, latitude) and environmental (temperature, salinity, chlorophyll *a*, nitrate, phosphate) variables. Panels: (a) longitude, (b) latitude, (c) SST, (d) salinity, (e) chlorophyll *a*, (f) nitrate, and (g) phosphate. Solid lines indicate fitted generalized additive models (GAMs), and shaded areas represent 95% confidence intervals. R^2 and *p*-values are shown in each panel. Statistical significance was assessed at $p < 0.05$.

Figure 8. Shannon diversity index of surface fungal communities in relation to geographic (longitude, latitude) and environmental (SST, salinity, chlorophyll a, nitrate, phosphate) variables. Panels: (a) longitude, (b) latitude, (c) SST, (d) salinity, (e) chlorophyll *a*, (f) nitrate, and (g) phosphate. Solid lines indicate fitted generalized additive models (GAMs), and shaded areas represent 95% confidence intervals. R^2 and *p*-values are displayed in each panel. Statistical significance was assessed at $p < 0.05$. SST, sea surface temperature.

Figure 9. Redundancy analysis (RDA) illustrating relationships between surface fungal community composition and environmental and geographic variables. Points represent individual surface samples, and arrows indicate the direction and strength of explanatory variables. The first and second constrained axes explained 6.63% and 3.32% of the total variation, respectively. Environmental variables included sea surface temperature (SST), salinity, chlorophyll *a*, nitrate, and phosphate, while geographic variables included longitude and latitude.

Figure 10. Predicted functional guild composition of fungal communities across water layers in the tropical Indian Ocean and western Pacific Ocean. Relative abundances of major fungal functional guilds were inferred using FUNGuild.

Figure 1.

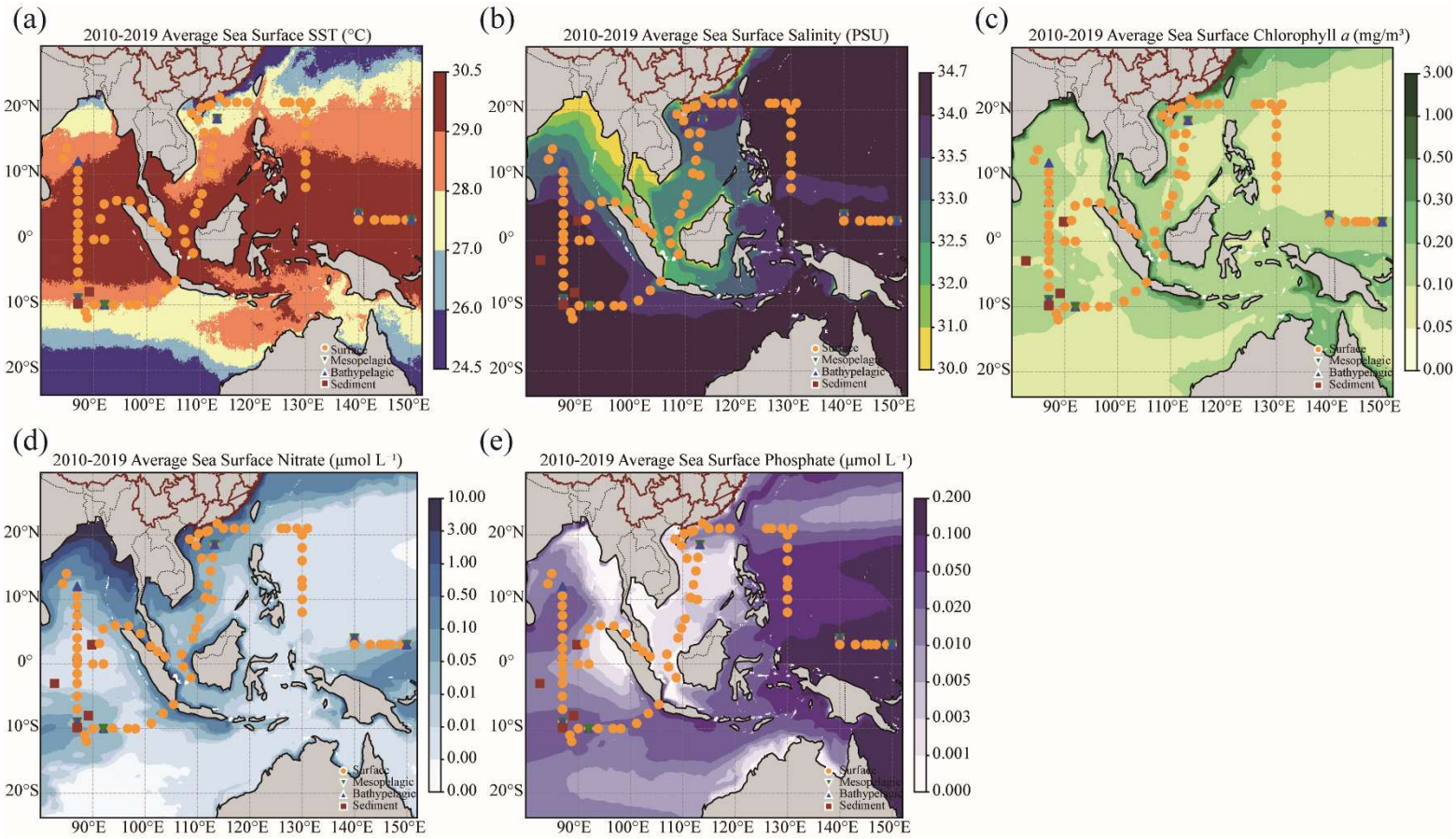
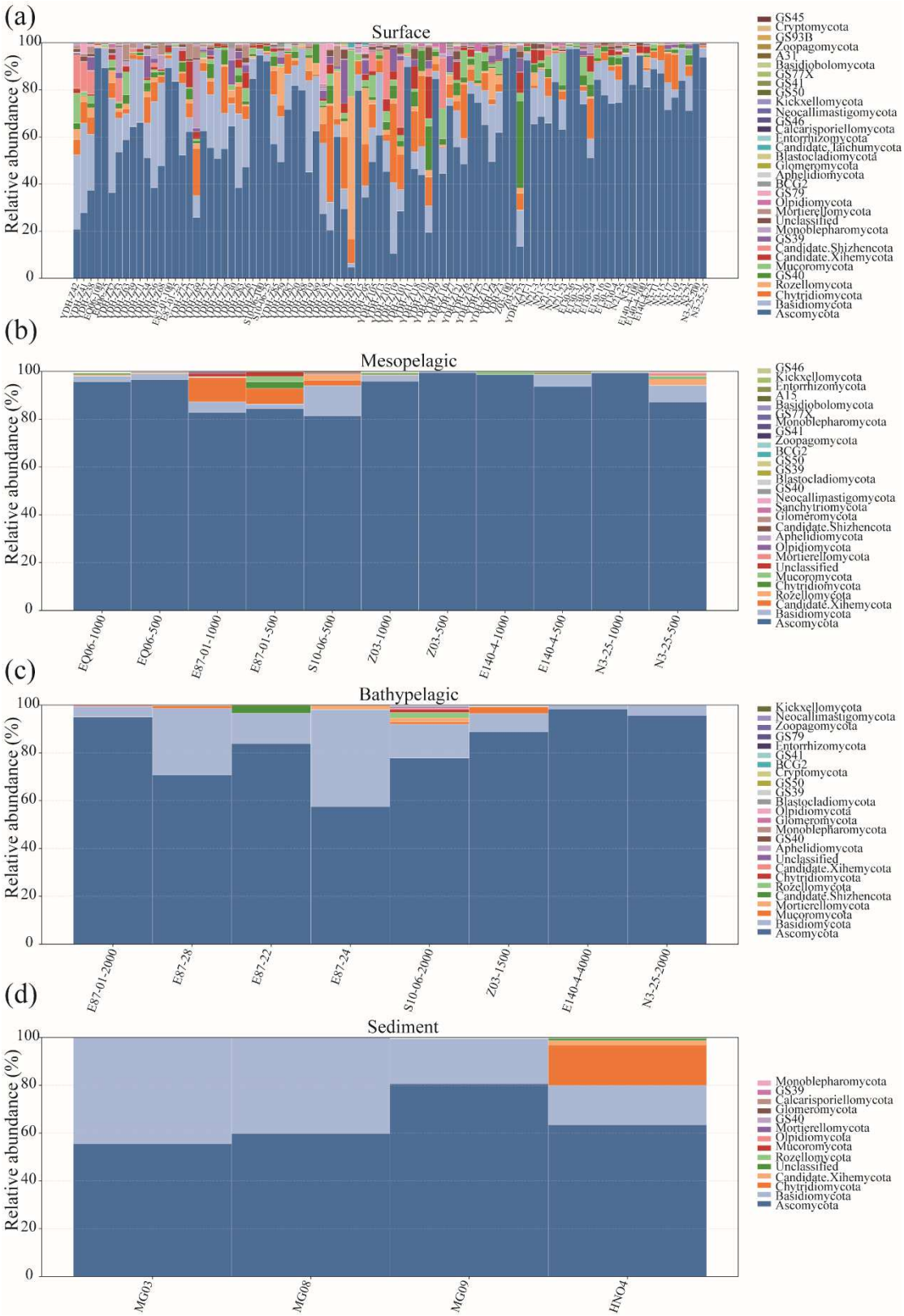

(a)
2010-2019 Average Sea Surface SST (°C)
30.5
29.0
28.0
27.0
26.0
24.5
(b)
2010-2019 Average Sea Surface Salinity (PSU)
34.7
34.0
33.5
33.0
32.5
32.0
31.0
30.0
(c)
2010-2019 Average Sea Surface Chlorophyll a (mg/m³)
3.00
1.00
0.50
0.30
0.20
0.10
0.05
0.00
(d)
2010-2019 Average Sea Surface Nitrate (μmol L ⁻¹)
10.00
3.00
1.00
0.50
0.10
0.05
0.01
0.01
0.00
0.00
(e)
2010-2019 Average Sea Surface Phosphate (μmol L ⁻¹)
0.200
0.100
0.050
0.020
0.010
0.005
0.003
0.001
0.000
20°N
10°N
0°
10°S
20°S
90°E 100°E 110°E 120°E 130°E 140°E 150°E
Surface
Mesopelagic
Bathypelagic
Sediment

Figure 2.


(a)
Surface
Relative abundance (%)
100
80
60
40
20
0
GS45
Cryptomycota
GS93B
Zoopagomycota
A31
Basidiobolomycota
GS77X
GS41
GS50
Kickxellomycota
Neocallimastigomycota
GS46
Calcarisporiellomycota
Entorrhizomycota
Candidate.Jaichumycota
Blastocladiomycota
Glomeromycota
Aphelidiomycota
BCG2
GS79
Olpidiomycota
Mortierellomycota
Unclassified
Monoblepharomycota
GS39
Candidate.Shizhencota
Candidate.Xihemycota
Mucoromycota
GS40
Rozellomycota
Chytridiomycota
Basidiomycota
Ascomycota
(b)
Mesopelagic
Relative abundance (%)
EQ06-1000
EQ06-500
E87-01-1000
E87-01-500
S10-06-500
Z03-1000
Z03-500
E140-4-1000
E140-4-500
N3-25-1000
N3-25-500
GS46
Kickxellomycota
Entorrhizomycota
A15
Basidiobolomycota
GS77X
Monoblepharomycota
GS41
Zoopagomycota
BCG2
GS50
GS39
Blastocladiomycota
GS40
Neocallimastigomycota
Sanchytriomycota
Glomeromycota
Candidate.Shizhencota
Aphelidiomycota
Olpidiomycota
Mortierellomycota
Unclassified
Mucoromycota
Chytridiomycota
Rozellomycota
Candidate.Xihemycota
Basidiomycota
Ascomycota
(c)
Bathypelagic
Relative abundance (%)
E87-01-2000
E87-28
E87-22
E87-24
S10-06-2000
Z03-1500
E140-4-4000
N3-25-2000
Kickxellomycota
Neocallimastigomycota
Zoopagomycota
GS79
Entorrhizomycota
GS41
BCG2
Cryptomycota
GS50
GS39
Blastocladiomycota
Olpidiomycota
Glomeromycota
Monoblepharomycota
GS40
Aphelidiomycota
Unclassified
Candidate.Xihemycota
Chytridiomycota
Rozellomycota
Candidate.Shizhencota
Mortierellomycota
Mucoromycota
Basidiomycota
Ascomycota
(d)
Sediment
Relative abundance (%)
MG03
MG08
MG09
HN04
Monoblepharomycota
GS39
Calcarisporiellomycota
Glomeromycota
GS40
Mortierellomycota
Olpidiomycota
Mucoromycota
Rozellomycota
Unclassified
Candidate.Xihemycota
Chytridiomycota
Basidiomycota
Ascomycota

991

992 **Figure 3.**

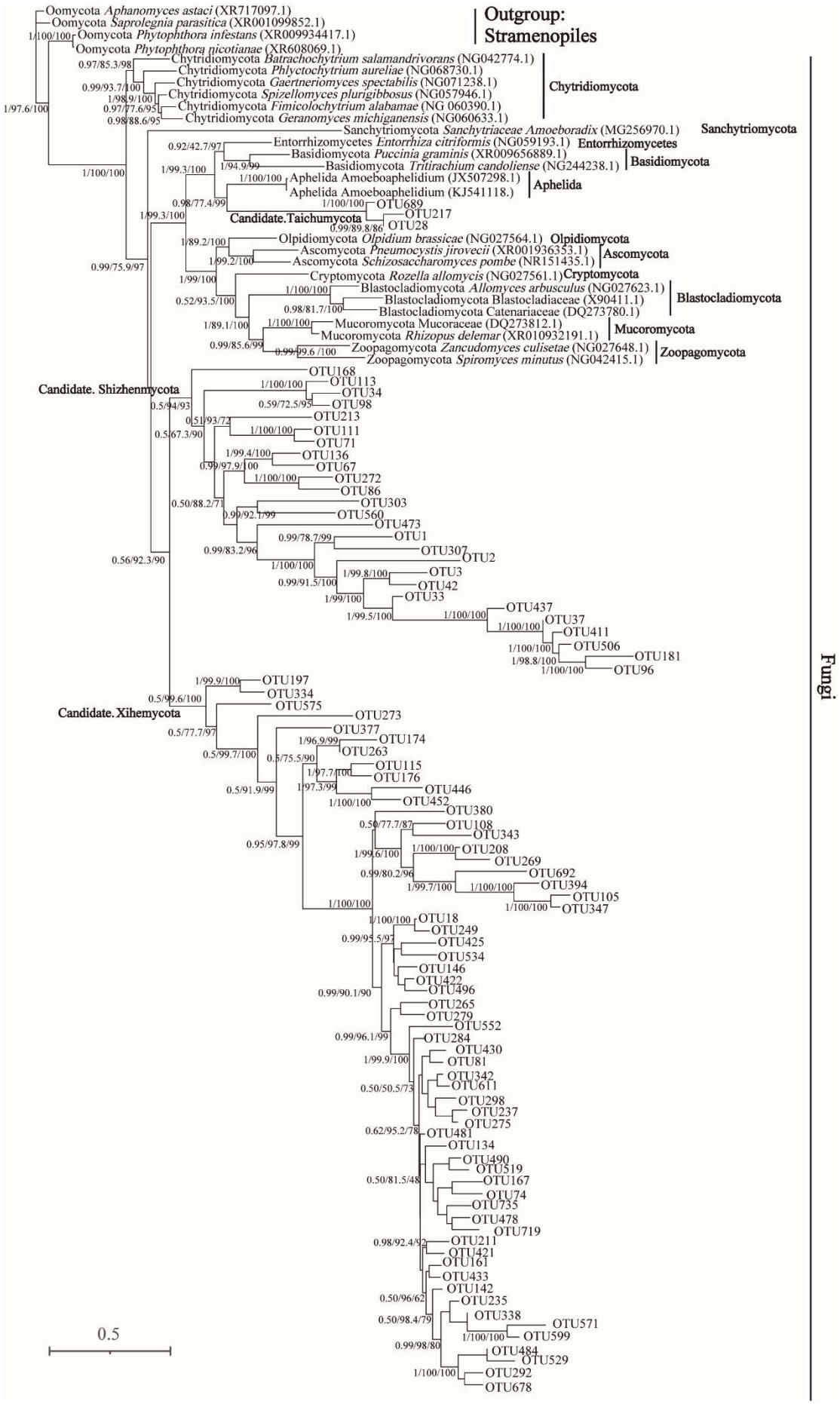

Outgroup:
Stramenopiles
Oomycota Aphanomyces astaci (XR717097.1)
Oomycota Saprolegnia parasitica (XR001099852.1)
Oomycota Phytophthora infestans (XR009934417.1)
Oomycota Phytophthora nicotianae (XR608069.1)
Chytridiomycota Batrachochytrium salamandrivorans (NG042774.1)
Chytridiomycota Phlyctochytrium aureliae (NG068730.1)
Chytridiomycota Gaertneriomyces spectabilis (NG071238.1)
Chytridiomycota Spizellomyces plurigibbosus (NG057946.1)
Chytridiomycota Fimicolochytrium alabamae (NG 060390.1)
Chytridiomycota Geranomyces michiganensis (NG060633.1)
Chytridiomycota
Sanchytriomycota Sanchytriaceae Amoeboradix (MG256970.1)
Sanchytriomycota
Entorrhizomycetes Entorrhiza citriformis (NG059193.1)
Entorrhizomycetes
Basidiomycota Puccinia graminis (XR009656889.1)
Basidiomycota Tritirachium candoliense (NG244238.1)
Basidiomycota
Aphelida Amoeboaphelidium (JX507298.1)
Aphelida Amoeboaphelidium (KJ541118.)
Aphelida
OTU689
OTU217
Candidate.Taichumycota
OTU28
Olpidiomycota Olpidium brassicae (NG027564.1)
Olpidiomycota
Ascomycota Pneumocystis jirovecii (XR001936353.1)
Ascomycota Schizosaccharomyces pombe (NR151435.1)
Ascomycota
Cryptomycota Rozella allomycis (NG027561.1)
Cryptomycota
Blastocladiomycota Allomyces arbusculus (NG027623.1)
Blastocladiomycota Blastocladiaceae (X90411.1)
Blastocladiomycota Catenariaceae (DQ273780.1)
Blastocladiomycota
Mucoromycota Mucoraceae (DQ273812.1)
Mucoromycota Rhizopus delemar (XR010932191.1)
Mucoromycota
Zoopagomycota Zancudomyces culisetae (NG027648.1)
Zoopagomycota Spiromyces minutus (NG042415.1)
Zoopagomycota
OTU168
OTU113
OTU34
Candidate. Shizhenmycota
OTU98
OTU213
OTU111
OTU71
OTU136
OTU67
OTU272
OTU86
OTU303
OTU560
OTU473
OTU1
OTU307
OTU2
OTU3
OTU42
OTU33
OTU437
OTU37
OTU411
OTU506
OTU181
OTU96
OTU197
OTU334
Candidate. Xihemycota
OTU575
OTU273
OTU377
OTU174
OTU263
OTU115
OTU176
OTU446
OTU452
OTU380
OTU108
OTU343
OTU208
OTU269
OTU692
OTU394
OTU105
OTU347
OTU18
OTU249
OTU425
OTU534
OTU146
OTU422
OTU496
OTU265
OTU279
OTU552
OTU284
OTU430
OTU81
OTU342
OTU611
OTU298
OTU237
OTU275
OTU481
OTU134
OTU490
OTU519
OTU167
OTU74
OTU735
OTU478
OTU719
OTU211
OTU421
OTU161
OTU433
OTU142
OTU235
OTU338
OTU571
OTU599
OTU484
OTU529
OTU292
OTU678
0.5
Fungi

Figure 4.

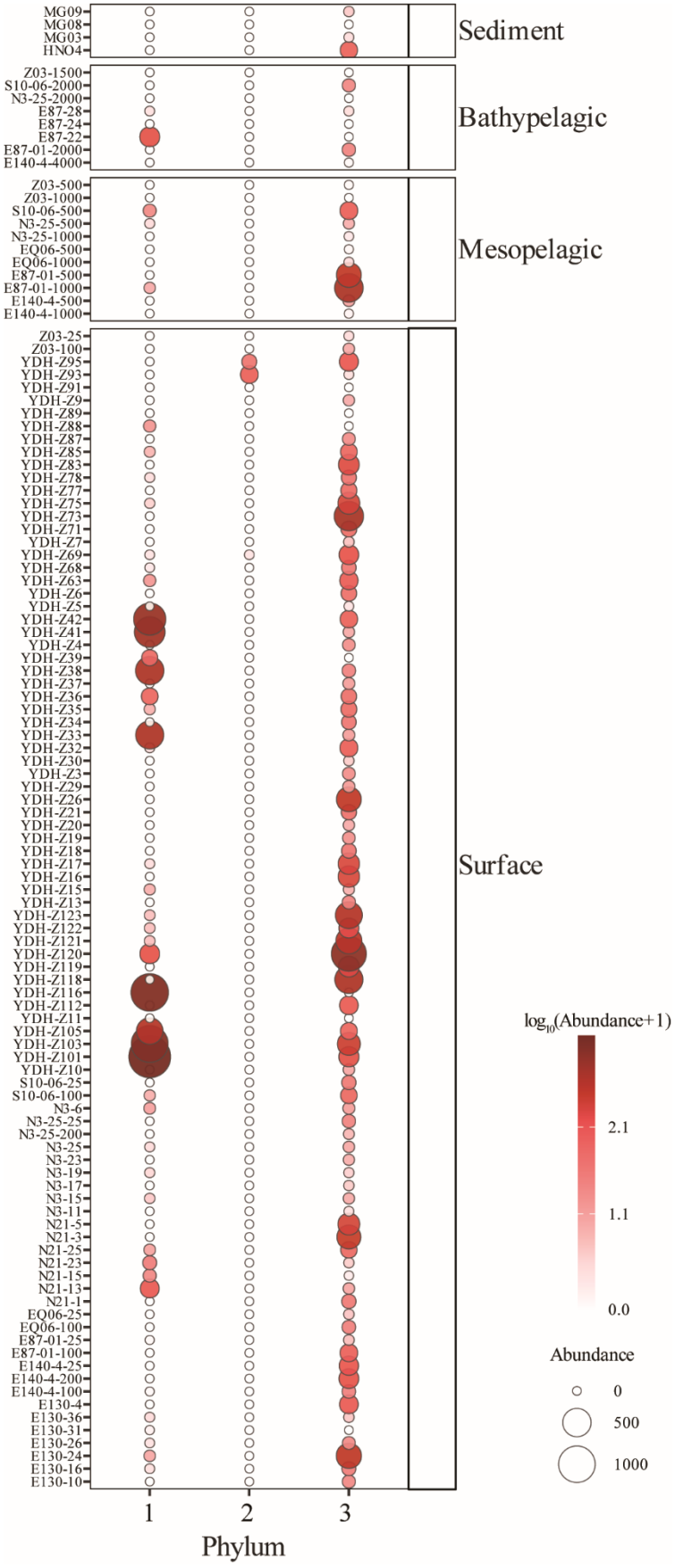

MG09
MG08
MG03
HNO4
Sediment
Z03-1500
S10-06-2000
N3-25-2000
E87-28
E87-24
E87-22
E87-01-2000
E140-4-4000
Bathypelagic
Z03-500
Z03-1000
S10-06-500
N3-25-500
N3-25-1000
EQ06-500
EQ06-1000
E87-01-500
E87-01-1000
E140-4-500
E140-4-1000
Mesopelagic
Z03-25
Z03-100
YDH-Z95
YDH-Z93
YDH-Z91
YDH-Z9
YDH-Z89
YDH-Z88
YDH-Z87
YDH-Z85
YDH-Z83
YDH-Z78
YDH-Z77
YDH-Z75
YDH-Z73
YDH-Z71
YDH-Z7
YDH-Z69
YDH-Z68
YDH-Z63
YDH-Z6
YDH-Z5
YDH-Z42
YDH-Z41
YDH-Z4
YDH-Z39
YDH-Z38
YDH-Z37
YDH-Z36
YDH-Z35
YDH-Z34
YDH-Z33
YDH-Z32
YDH-Z30
YDH-Z3
YDH-Z29
YDH-Z26
YDH-Z21
YDH-Z20
YDH-Z19
YDH-Z18
YDH-Z17
YDH-Z16
YDH-Z15
YDH-Z13
YDH-Z123
YDH-Z122
YDH-Z121
YDH-Z120
YDH-Z119
YDH-Z118
YDH-Z116
YDH-Z112
YDH-Z11
YDH-Z105
YDH-Z103
YDH-Z101
YDH-Z10
S10-06-25
S10-06-100
N3-6
N3-25-25
N3-25-200
N3-25
N3-23
N3-19
N3-17
N3-15
N3-11
N21-5
N21-3
N21-25
N21-23
N21-15
N21-13
N21-1
EQ06-25
EQ06-100
E87-01-25
E87-01-100
E140-4-25
E140-4-200
E140-4-100
E130-4
E130-36
E130-31
E130-26
E130-24
E130-16
E130-10
Surface
1
2
3
Phylum
log10(Abundance+1)
2.1
1.1
0.0
Abundance
0
500
1000

Figure 5.

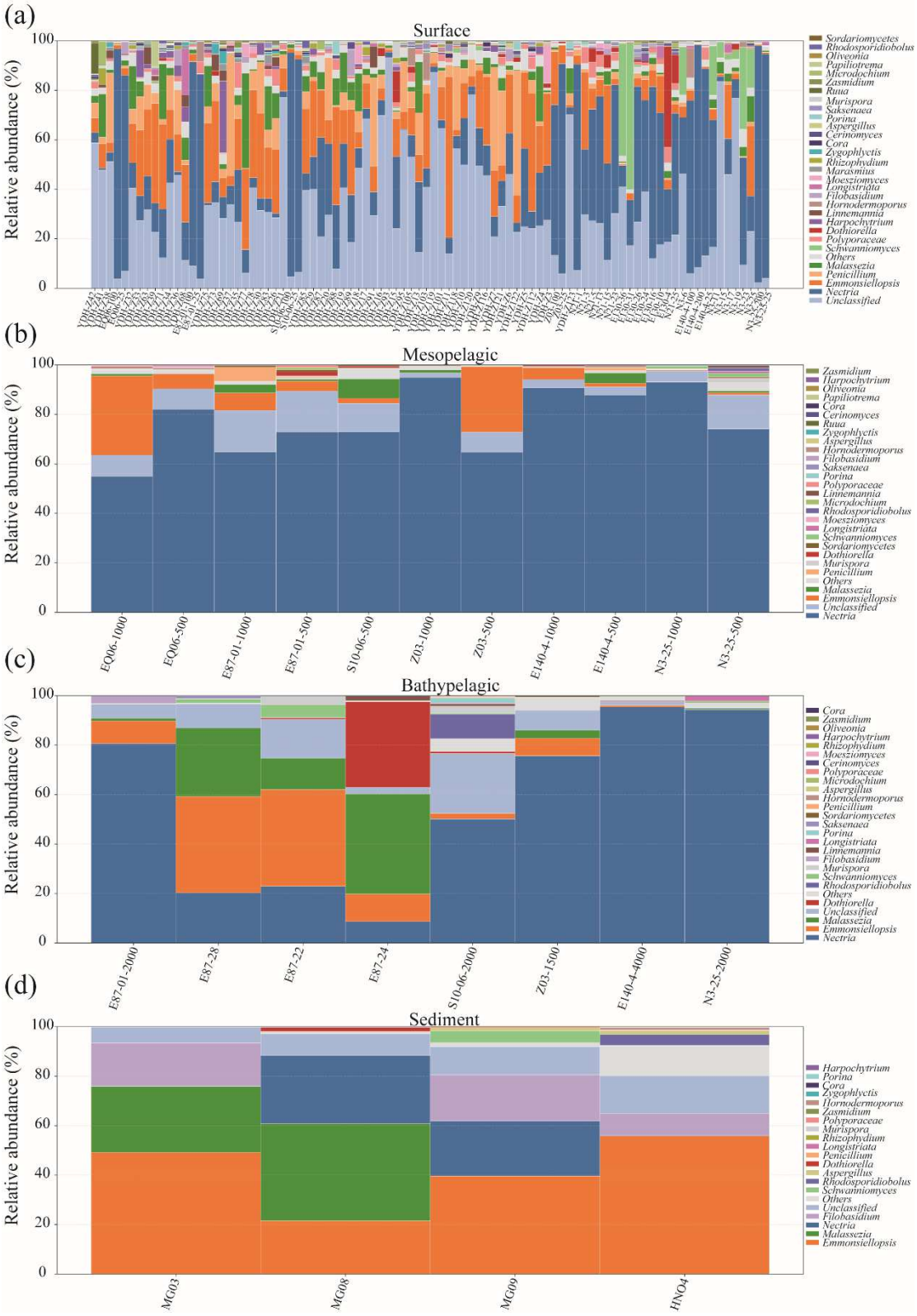

(a)
Surface
Relative abundance (%)
100
80
60
40
20
0
Sordariomycetes
Rhodosporidiobolus
Oliveonia
Papiliotrema
Microdochium
Zasmidium
Rusa
Murispora
Saksenaea
Porina
Aspergillus
Cerinomyces
Cora
Zygophlyctis
Rhizophydium
Marasmius
Moesziomyces
Longistriata
Filobasidium
Hornodermoporus
Linnemannia
Harpochytrium
Dothiorella
Polyporaceae
Schwanniomyces
Others
Malassezia
Penicillium
Emmonsiellopsis
Nectria
Unclassified
(b)
Mesopelagic
Relative abundance (%)
EQ06-1000
EQ06-500
E87-01-1000
E87-01-500
S10-06-500
Z03-1000
Z03-500
E140-4-1000
E140-4-500
N3-25-1000
N3-25-500
Zasmidium
Harpochytrium
Oliveonia
Papiliotrema
Cora
Cerinomyces
Rusa
Zygophlyctis
Aspergillus
Hornodermoporus
Filobasidium
Saksenaea
Porina
Polyporaceae
Linnemannia
Microdochium
Rhodosporidiobolus
Moesziomyces
Longistriata
Schwanniomyces
Sordariomycetes
Dothiorella
Murispora
Penicillium
Others
Malassezia
Emmonsiellopsis
Unclassified
Nectria
(c)
Bathypelagic
Relative abundance (%)
E87-01-2000
E87-28
E87-22
E87-24
S10-06-2000
Z03-1500
E140-4-4000
N3-25-2000
Cora
Zasmidium
Oliveonia
Harpochytrium
Rhizophydium
Moesziomyces
Cerinomyces
Polyporaceae
Microdochium
Aspergillus
Hornodermoporus
Penicillium
Sordariomycetes
Saksenaea
Porina
Longistriata
Linnemannia
Filobasidium
Murispora
Schwanniomyces
Rhodosporidiobolus
Others
Dothiorella
Unclassified
Malassezia
Emmonsiellopsis
Nectria
(d)
Sediment
Relative abundance (%)
MG03
MG08
MG09
HNO4
Harpochytrium
Porina
Cora
Zygophlyctis
Hornodermoporus
Zasmidium
Polyporaceae
Murispora
Rhizophydium
Longistriata
Penicillium
Dothiorella
Aspergillus
Rhodosporidiobolus
Schwanniomyces
Others
Unclassified
Filobasidium
Nectria
Malassezia
Emmonsiellopsis

Figure 6.

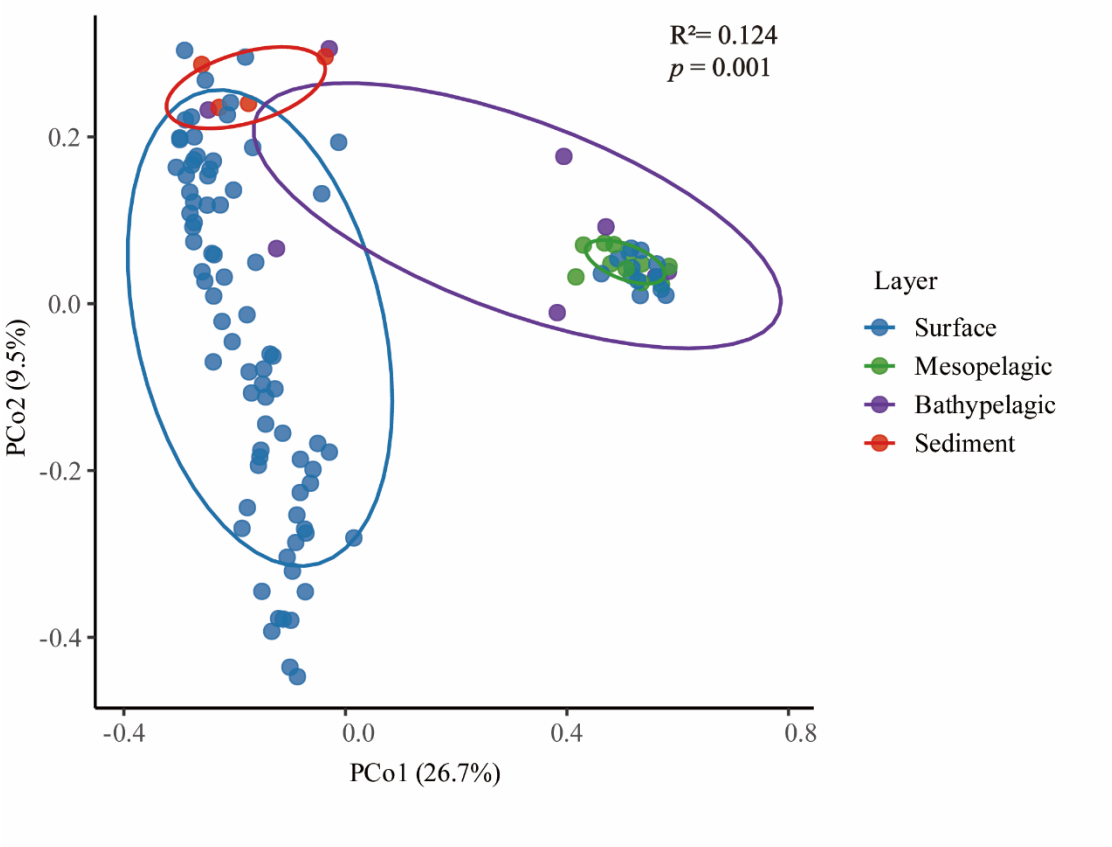

R²= 0.124
p = 0.001
0.2
0.0
-0.2
-0.4
PCo2 (9.5%)
-0.4
0.0
0.4
0.8
PCo1 (26.7%)
Layer
Surface
Mesopelagic
Bathypelagic
Sediment

Figure 7.

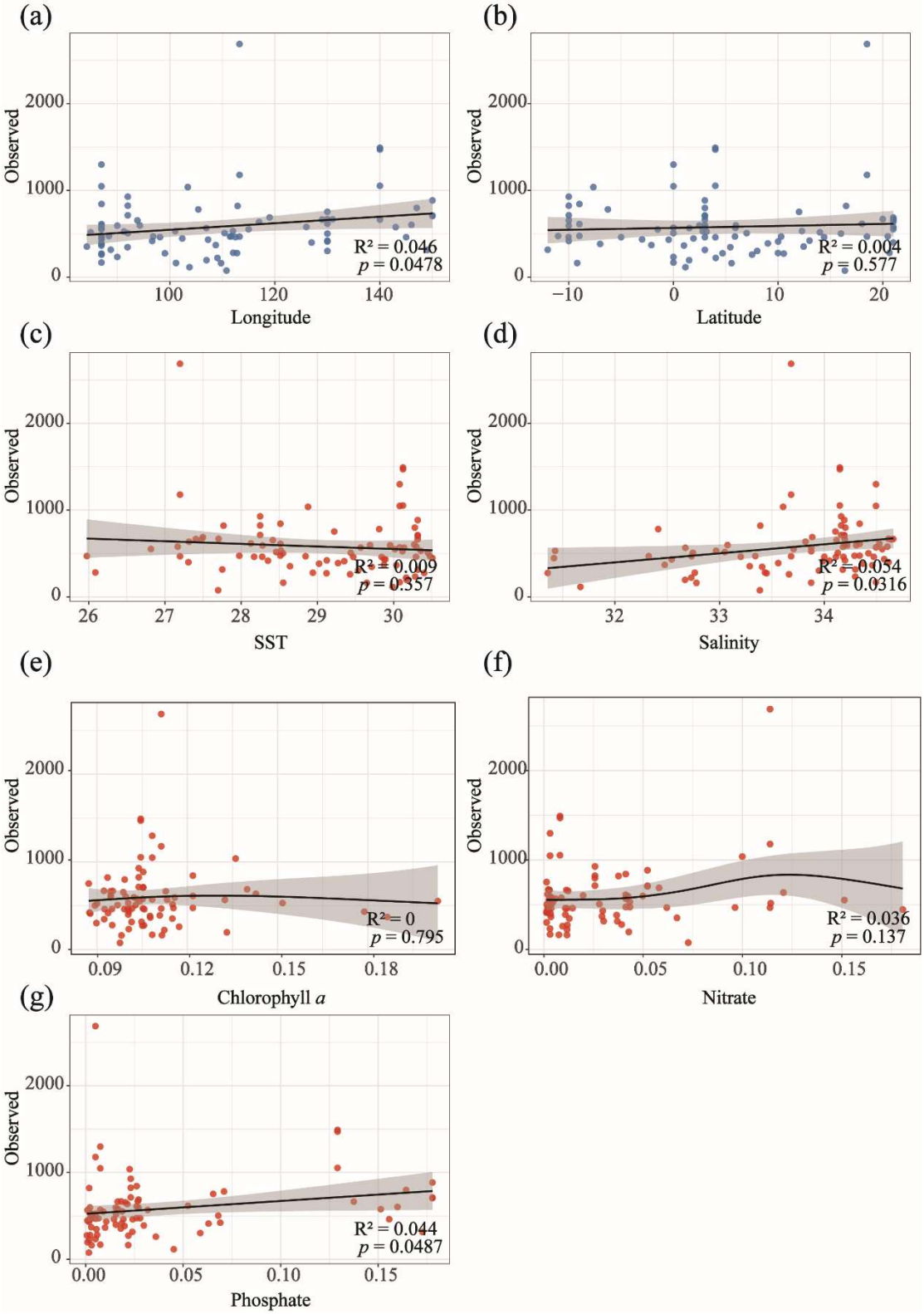

(a)
Observed
2000
1000
0
100
120
140
Longitude
R² = 0.046
p = 0.0478
(b)
Observed
2000
1000
0
−10
0
10
20
Latitude
R² = 0.004
p = 0.577
(c)
Observed
2000
1000
0
26
27
28
29
30
SST
R² = 0.009
p = 0.357
(d)
Observed
2000
1000
0
32
33
34
Salinity
R² = 0.054
p = 0.0316
(e)
Observed
2000
1000
0
0.09
0.12
0.15
0.18
Chlorophyll a
R² = 0
p = 0.795
(f)
Observed
2000
1000
0
0.00
0.05
0.10
0.15
Nitrate
R² = 0.036
p = 0.137
(g)
Observed
2000
1000
0
0.00
0.05
0.10
0.15
Phosphate
R² = 0.044
p = 0.0487

Figure 8.

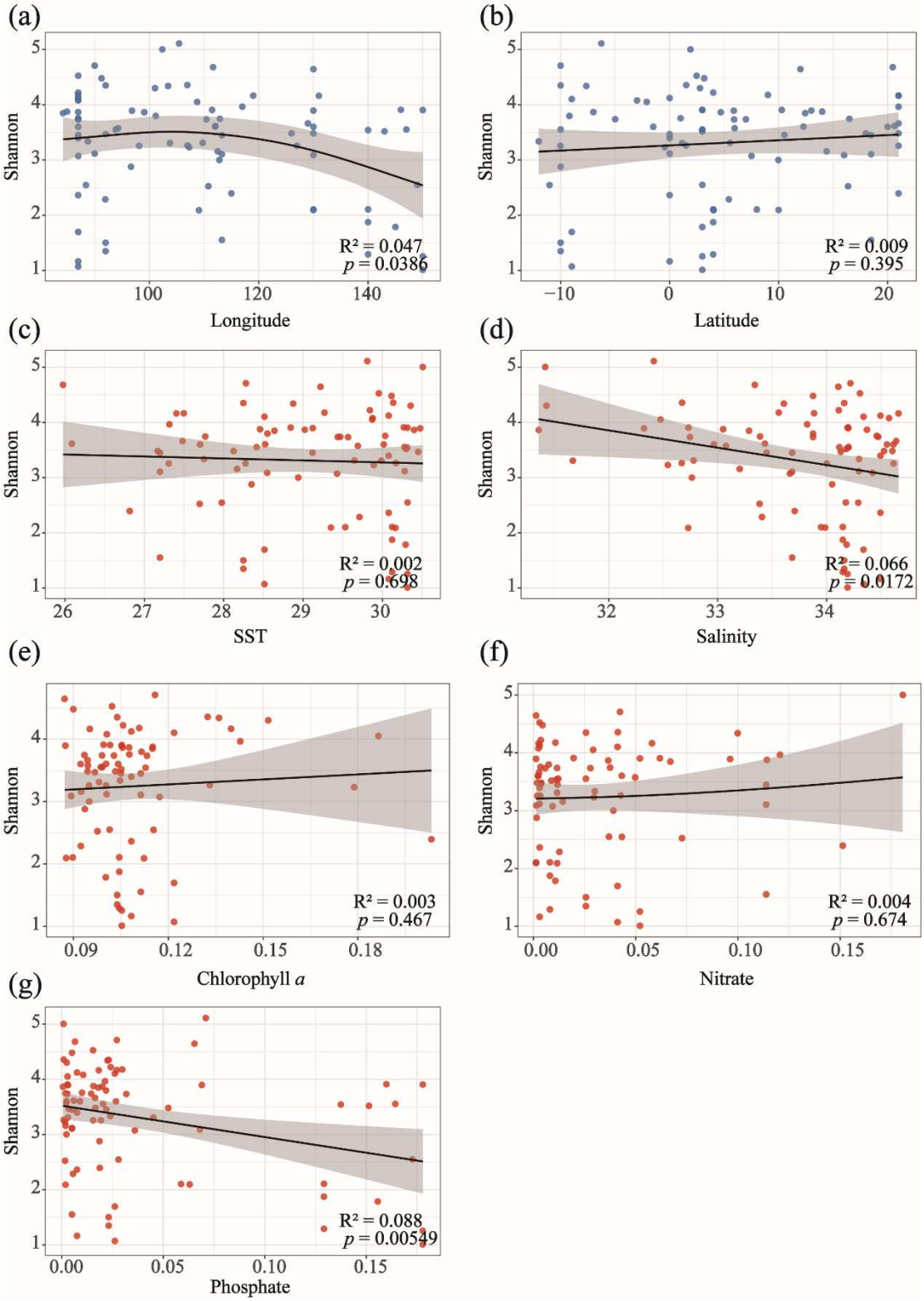
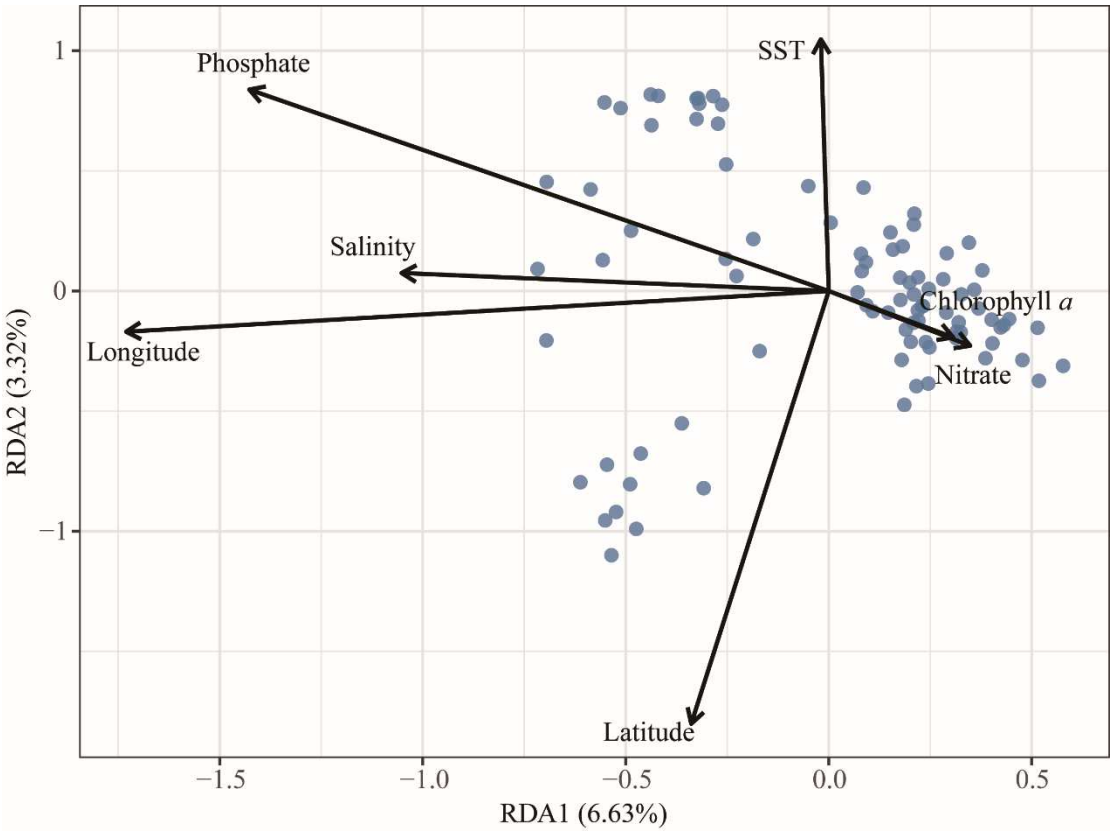
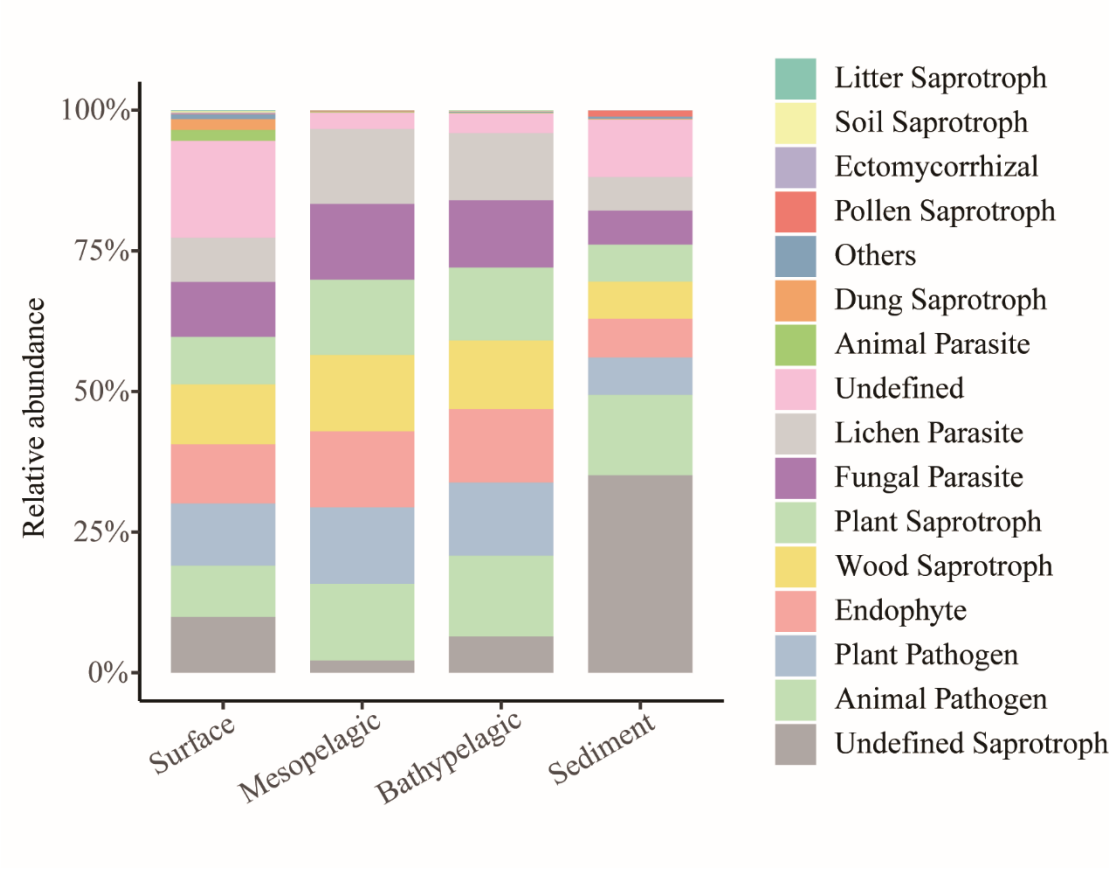

(a)
Shannon
Longitude
R² = 0.047
p = 0.0386
(b)
Shannon
Latitude
R² = 0.009
p = 0.395
(c)
Shannon
SST
R² = 0.002
p = 0.698
(d)
Shannon
Salinity
R² = 0.066
p = 0.0172
(e)
Shannon
Chlorophyll a
R² = 0.003
p = 0.467
(f)
Shannon
Nitrate
R² = 0.004
p = 0.674
(g)
Shannon
Phosphate
R² = 0.088
p = 0.00549

Figure 9.


Phosphate
SST
Salinity
Chlorophyll *a*
Longitude
Nitrate
Latitude
RDA2 (3.32%)
RDA1 (6.63%)
1
0
−1
−1.5
−1.0
−0.5
0.0
0.5

1037 **Figure 10.**



1038

Supplementary Files

This is a list of supplementary files associated with this preprint. Click to download.

- Additionalfile1insitumetadata.xlsx
- Additionalfile2decadalaverageenvironmentalmetadata.csv
- Additionalfile3custom28Sfungaldatabase.fasta
- Additionalfile4analysiscode.docx
- Additionalfile5allOTUstaxonomyraw.csv
- Additionalfile6fungalOTUstaxonomyraw.csv
- Additionalfile7bioinformaticsprocessingsummary.csv
- Additionalfile8relativeabundancefungalphylabywaterlayer.csv
- Additionalfile9relativeabundancefungalgenusbywaterlayer.csv
- Additionalfile10alphadiversitybysample.csv
- Additionalfile11FUNGuildpredictions.csv
- Additionalfile12relativeabundancefungalfunctionalguildsbywaterlayer.csv
- Supplementaryfiles.docx